Lamb wave evaluation of concrete plates

Tofeldt, Oskar

Published: 2017-09-01

Document Version
Publisher's PDF, also known as Version of record

Link to publication

Lamb wave evaluation of concrete plates

Oskar Tofeldt

LUND UNIVERSITY

DOCTORAL DISSERTATION
by due permission of the Faculty of Engineering, Lund University, Sweden.

To be defended at the Faculty of Engineering (LTH),
E-building, room E:B, Ole Römers väg 3, Lund,
on September 28, 2017, at 10.00 a.m.

Faculty opponent
Dr. Odile Abraham
Geophysics and Non Destructive Evaluation Laboratory,
IFSTTAR, The French institute of science and technology for transport,
development and networks.

Organization: LUND UNIVERSITY Faculty of Engineering Division of Engineering Geology Box 118, SE-22100 Lund, Sweden	**Document name:** DOCTORAL THESIS
	Date of issue: 2017-09-01
Author: Oskar Tofeldt	**Sponsoring organizations:** The Development Fund of the Swedish Construction Industry (SBUF) through Peab and The Swedish Radiation Safety Authority (SSM).

Title: Lamb wave evaluation of concrete plates

Abstract:
This thesis is about the application of Lamb waves for non-destructive evaluation of plate-like concrete structures under one-sided access test condition using a portable equipment consisting of an accelerometer and impact hammer. With this type of equipment and based on array signal processing, the impact-echo (IE) method can be extended with measurements of surface waves; this extension allows an evaluation with Lamb waves. For both the conventional impact-echo method as well as evaluations based on Lamb waves, results in the literature report a systematically underestimated plate thickness. This error is investigated and reproduced in a numerical study and further verified in a measurement. A main source of uncertainty is related to the estimation of a longitudinal wave velocity from first arrivals. To reduce this uncertainty, a new approach for estimation of Poisson's ratio is proposed. The new approach is based on the amplitude polarization of the S1-ZGV Lamb mode: a through-thickness representative estimate of Poisson's ratio is thereby obtained leading to an overall improved estimation of the Lamb wave plate parameters.

A new technique based on 2D arrays is also presented. In an example, the technique is used to map (image) the variation of phase velocity for the A0 Lamb mode in the lateral plane of the plate; that is, the technique is in this case used to assess the material and plate thickness homogeneity. Compared to ultrasonic reflection imaging methods, no limitation to a specific set of operating frequencies (transducers) exists since the 2D array technique is based on a full wave field dataset with wide frequency bandwidth. Variation of material properties transversally through the thickness may also exist. For improved understanding about zero-group velocity (ZGV) modes under this type of material condition, two cases with continuously varying acoustic bulk wave velocities are investigated. Results show that a zero-group velocity mode exists with the similar robustness and detectability for both cases: non-destructive applications based on zero-group velocity modes are possible also for these two material variation cases.

Key words: Lamb waves; guided waves; impact-echo; concrete; non-destructive evaluation.

Classification system and/or index terms (if any):		
Supplementary bibliographical information:		**Language:** English
ISSN and key title: ISRN LUTVDG/(TVTG-1038)/1-144/(2017)		**ISBN:** 978-91-7753-379-5 (Print), 978-91-7753-380-1 (Electronic)
Recipient's notes	**Number of pages:** 144	**Price:** 110 SEK
	Security classification:	

Lamb wave evaluation of concrete plates

Oskar Tofeldt
oskar.tofeldt@tg.lth.se

Doctoral Thesis
2017

Division of Engineering geology, Lund University
Box 118, SE-221 00 Lund, Sweden

ISBN 978-91-7753-379-5 (Print)
ISBN 978-91-7753-380-1 (PDF)

ISRN LUTVDG/(TVTG-1038)/1-144/(2017)

List of papers

This thesis is composed by the following papers:

Paper I O. Baggens and N. Ryden. 2015.
Systematic errors in Impact-Echo thickness estimation due to near field effects. NDT & E International, 69:16-27.
DOI: 10.1016/j.ndteint.2014.09.003.

Paper II O. Baggens and N. Ryden. 2015.
Poisson's ratio from polarization of acoustic zero-group velocity Lamb mode. The Journal of the Acoustical Society of America, 138(1):EL88-EL92.
DOI: 10.1121/1.4923015.

Paper III O. Tofeldt and N. Ryden. 2017.
Lamb wave phase velocity imaging of concrete plates with 2D-arrays. Under review, Journal of Nondestructive Evaluation.

Paper IV O. Tofeldt and N. Ryden. 2017.
Zero-group velocity modes in plates with continuous material variation through the thickness. The Journal of the Acoustical Society of America, 141(5):3302-3311.
DOI: 10.1121/1.4983296

Authors' contributions

All simulations were performed by Tofeldt (previously Baggens) with advice from Ryden. The measurement in Paper 1 was planned and performed by Ryden. The measurements in Paper 2 and Paper 3 were planned and performed by Tofeldt (Baggens) with advice from Ryden. Data from all simulations and measurements were processed and analyzed by Tofeldt (Baggens) with guidance by Ryden. Tofeldt (Baggens) prepared the figures, wrote and submitted all papers and acted as corresponding author. Ryden supported with advice, feedback and comments during the work with the papers.

Related publications

O. Baggens and N. Ryden. 2015.
Near field effects and estimation of Poisson's ratio in impact-echo thickness testing. 41st annual Review of Progress in Quantitative Non-Destructive Evaluation, QNDE Boise 2014. AIP Conference Proceedings 1650, 1415 (2015)
DOI: 10.1063/1.4914757.

O. Baggens and N. Ryden. 2015.
Lamb Wave Plate Parameters from Combined Impact-Echo and Surface Wave Measurement. International Symposium in Non-Destructive Testing in Civil Engineering, NDT-CE Berlin 2015.
http://www.ndt.net/article/ndtce2015/papers/103_baggens_oskar.pdf

O. Baggens. 2015.
Non-destructive evaluation of plate-like concrete structures: elastic properties and thickness. Licentiate thesis, Lund University, Sweden.
ISBN: 978-91-7623-259-0 (print), 978-91-7623-260-6 (electronic/pdf).

Abstract

This thesis is about the application of Lamb waves for non-destructive evaluation of plate-like concrete structures under one-sided access test condition using a portable equipment consisting of an accelerometer and impact hammer. With this type of equipment and based on array signal processing, the impact-echo (IE) method can be extended with measurements of surface waves; this extension allows an evaluation with Lamb waves. For both the conventional impact-echo method as well as evaluations based on Lamb waves, results in the literature report a systematically underestimated plate thickness. This error is investigated and reproduced in a numerical study and further verified in a measurement. A main source of uncertainty is related to the estimation of a longitudinal wave velocity from first arrivals. To reduce this uncertainty, a new approach for estimation of Poisson's ratio is proposed. The new approach is based on the amplitude polarization of the S1-ZGV Lamb mode: a through-thickness representative estimate of Poisson's ratio is thereby obtained leading to an overall improved estimation of the Lamb wave plate parameters.

A new technique based on 2D arrays is also presented. In an example, the technique is used to map (image) the variation of phase velocity for the A0 Lamb mode in the lateral plane of the plate; that is, the technique is in this case used to assess the material and plate thickness homogeneity. Compared to ultrasonic reflection imaging methods, no limitation to a specific set of operating frequencies (transducers) exists since the 2D array technique is based on a full wave field dataset with wide frequency bandwidth. Variation of material properties transversally through the thickness may also exist. For improved understanding about zero-group velocity (ZGV) modes under this type of material condition, two cases with continuously varying acoustic bulk wave velocities are investigated. Results show that a zero-group velocity mode exists with the similar robustness and detectability for both cases: non-destructive applications based on zero-group velocity modes are possible also for these two material variation cases.

Populärvetenskaplig sammafattning

Betong är ett av världens vanligaste byggnadsmaterial. Det används ofta i konstruktioner som broar, hamnar, tunnlar och kraftverk. Att kunna undersöka och bedöma tillståndet hos dessa typer av konstruktioner, ungefär som en hälsokontroll, är viktigt för säker drift och användning. Detta gäller speciellt när konstruktionerna blir äldre. Samtidigt bör inte undersökningarna orsaka skador på konstruktionerna. Det är därför viktigt med undersökningsmetoder baserade på oförstörande provning eftersom oförstörande provning inte orsakar skador vid undersökning av konstruktioner.

Oförstörande provning kan även användas för kvalitetskontroll vid nyproduktion, men också för att underlätta och planera underhåll. Därmed är oförstörande provning viktig för att uppnå effektivt resursutnyttjande och ur ett hållbart-utvecklings perspektiv. Den här avhandlingen handlar om förbättring och vidareutveckling av en metod för oförstörande provning som används för att utvärdera mekaniska egenskaper i betongkonstruktioner. De nya förbättringarna kan även användas vid oförstörande provning av andra material än betong.

Ett materials mekaniska egenskaper beskriver hur materialet beter sig under belastning. Mekaniska egenskaperna kan utvärderas genom att analysera vibrationer i form av mekaniska vågor, en typ av ljudvågor. Ljudvågorna kan ha olika längd, så kallad våglängd. Våglängden har betydelse då betongkonstruktioner består av cement, grus, sten och armeringsjärn. Korta ljudvågor kan studsa kors och tvärs på grund av gruset, stenarna och armeringsjärnen. Det gör analysen svårare. Dessutom tystnar kortare ljudvågor efter en kortare sträcka jämfört med långa ljudvågor vilket minskar räckvidden. Dessa svårigheter uppkommer till exempel vid undersökning av stora betongkonstruktioner som broar och kraftverk. Arbetet i den här avhandlingen fokuserar därför på en metod där våglängden enkelt kan anpassas efter behov.

Ljudvågor i en konstruktion kan enkelt skapas genom att slå på betong-en med en hammare. Ljudvågorna kan sedan mätas med en accelerometer. Accelerometern kan ses som en typ av mikrofon. Arbetet i avhandlingen fokuserar på hur de inspelade ljudvågorna från accelerometern kan analyseras på bästa sätt. Bland annat mäts hur snabbt ljudvågorna färdas i konstruktionen. Hastigheten ger information om de mekaniska egenskaperna då hastigheten är beroende av materialet. Eftersom många konstruktioner har platt-liknande form är extra fokus riktat mot ljudvågor i betongplattor. I plattor måste ljudvågorna samsas på ett begränsat utrymme. Detta gör att ljudvågorna tillsammans får en särskild struktur och utseende som beror både på de mekaniska egenskaperna och tjockleken hos plattan. Tillsammans med ljudhastighetkan ger det en förbättrad utvärdering av plattans mekaniska egenskaper och tjocklek.

I början av avhandlingen studeras även tillförlitligheten i befintliga metoder som använder hammare och accelerometer. I befintliga metoder förekommer ett systematiskt fel som generar osäkerhet i uppmätta egenskaper och tjocklek. Detta systematiska fel utreds och en alternativ lösning och ny utvärderingsmetod som minskar det systematiska felet föreslås. I avhandlingen presenteras även förslag på vidareutveckling och förbättringar av hur ljudvågor kan spelas in och utvärderas över en större volym och yta än vad som tidigare gjorts. Det samlade resultatet möjliggör en förbättrad utvärdering av de mekaniska egenskaper och tjocklek i plattliknande betongkonstruktioner. Resultaten bidrar också till en djupare förståelse för ljudvågors beteende och uppträdande i plattor. Detta utgör en grund för fortsatt utveckling av metoder inom oförstörande provning för konstruktioner i såväl betong som andra material.

Preface

The work of this thesis, which represent the work within a PhD project, has been carried out at the Division of Engineering Geology at Lund University. The financial support from The Development Fund of the Swedish Construction Industry (SBUF) through Peab and The Swedish Radiation Safety Authority (SSM) is gratefully acknowledged.

The background to the PhD project can be traced back to the so-called CONSAFESYS project, organized by Scanscot Technology, about non-destructive condition assessment of nuclear reactor containments. The CONSAFESYS project involved practical testing on the decommissioned nuclear power plant Barsebäck in Sweden. At Barsebäck, both impact-echo and combined impact-echo and surface wave measurements have been performed with successful results, but sometimes also with less successful results. The experiences gained from these results called for further studies and resulted in the start of this PhD project at which I was recruited as student. The focus within this PhD project has therefore been directed towards techniques for the application of non-destructive evaluation of thick (>1 m) plate-like concrete structures. However, in the beginning of the PhD project it was realized that practical testing on a 40 years old power plant (Barsebäck) represent an extremely difficult task, especially in work with development of new processing techniques. For this reason, the field cases in PhD project used for the practical measurements were instead located to structures outside the nuclear power plant with the aim of obtaining less complicated test environments.

In November 2014, I participated in a field campaign within CONSAFESYS and performed measurements on Barsebäck. The initial data analysis further verified the difficulty in interpreting results, and focus in the PhD project was therefore continued to be directed towards the development of fundamental understanding of Lamb wave evaluation for plate-like concrete structures. It can be mentioned that staff from BAM (Bundesanstalt für Materialforschung und -prüfung), Berlin, also participated and conducted measurements. Although not presented in this thesis, their results further verified the difficulty of seismic and ultrasonic measurements on nuclear

containment walls. Clearly, this highlights the complexity of evaluations of thick and heavily reinforce concrete walls such as reactor containments. From the positive view, this means that there are more interesting work still to be done for techniques based on Lamb waves as well as ultrasonics.

During the course of this work, Nils Ryden has been my main supervisor. My foremost appreciation is directed to him for the excellent guidance, support and help I have received consistently throughout the years working with this thesis. Thank you!

I would also like to thank my assisting supervisors: Björn Thunell at Scanscot Technology and Gerhard Barmen at Lund University. During the work with Paper I, the help and feedback from Prof. John Popovics as well as Prof. Michael Lowe is gratefully acknowledged. The staff at Peab in Trollhättan is acknowledged for generously providing access to the test site used in Paper III. I am also thankful towards Christian Nielsen who did a master thesis (under Nils Ryden's and my supervision) about semi-analytical finite element modelling; his work and experiences provided great help in the development of the model used for the theoretical study in Paper IV. The feedback and interest from the reference group associated with the PhD project is also appreciated.

I would also like to express my appreciation to my fellow PhD students and the staff at the Division of Engineering Geology. After moving to Trollhättan, I have also worked part time at the research environment Production Technology West (PTW) at University West, Trollhättan. Besides from getting another interesting and valuable perspective on applications of non-destructive evaluation, this has also been very nice since I have had the opportunity to work with my PhD thesis from the office of PTW as well. Thank you all at PTW!

A major part of the work with this thesis has also been performed from the office at home (first Norrköping, then later on Trollhättan), and I would like to thank our dog, Tesla, for being the most awesome companion and colleague; especially for the nice breaks in the forest in which huge amount of energy was recovered - thus allowing problems to be solved when returning back to the computer... Thanks also to my family for support and encouragement during my years of studying. Last, but at no means the least, I want to thank my wife, Linda, for help with the "Populärvetenskaplig sammanfattning" and especially for having great patience with me (almost) never getting this work finished... Linda, you are the best!

Oskar Tofeldt
Trollhättan, August 2017

Contents

List of papers **iii**
Authors' contributions iii

Related publications **v**

Abstract **vii**

Populärvetenskaplig sammafattning **ix**

Preface **xi**

1 Introduction **1**
1.1 Background 1
1.2 Motivation of work 2
1.3 Aim, objective and limitations 3
1.4 Contributions of thesis 3
1.5 Thesis outline 4

2 Related research **5**
2.1 General note 5
2.2 Ultrasonic techniques 5
2.3 Impact-echo method 6
2.4 Impact-echo and surface waves 9
2.5 Obtaining the Lamb wave plate parameters 10
2.6 Uncertainties and challenges 12

3 Elastic wave theory **17**
3.1 Infinite spaces 17
3.2 Half-spaces 18
3.3 Lamb waves 19

4 Numerical modelling **23**
4.1 Calculation of dispersion curves 23
4.2 Response due to point source excitation 23

5 Measurement equipment **27**

6 Results **31**
6.1 1D array measurements and analysis 31
6.2 2D array measurement and analysis 40
6.3 Theoretical study inhomogeneous plates 48

7 Conclusions **57**

8 Suggestions for further work **59**

9 Bibliography **61**

Appendices **71**

Brief overview **73**

A Paper I **75**

B Paper II **89**

C Paper III **97**

D Paper IV **117**

Chapter 1

Introduction

This thesis concerns the application of Lamb waves for non-destructive evaluation of plate-like concrete structures. The focus is directed towards evaluation techniques based on full wave field datasets with wide-band frequency content measured with a light portable equipment consisting of an impact hammer, an accelerometer and a data acquisition card.

1.1 Background

Concrete is a commonly used construction material and plays an important role in roads, bridges, houses, power plants, etc. Many of these structures are getting older and begin to reach the end of their expected lifetime in operation. For this reason, there is an increasing need for techniques capable of verifying structural status and integrity to ensure safety in operation; ideally, if possible, the usage of techniques based on non-destructive evaluation (NDE) is favourable. Thus, in this process, techniques based on non-destructive evaluation represent a key part (Bungey et al., 2006). Also, in view of higher demands for sustainable use of resources, the value of such techniques become even more important since obtained data can facilitate maintenance as well as provide information that can be used in quality assurance systems (Maser, 2003; Deacon et al., 1997). A general definition of non-destructive evaluation is the task of evaluating some sort of property without introducing any permanent damage on the studied object (Shull, 2002). Although non-destructive evaluation techniques can appear in a number of different forms, the general principle of all techniques is essentially the same; indirect measured field quantities such as temperature, acceleration or pressure are, by means of physical principles, models and assumptions, translated to a form that provide increased knowledge concerning the initial question that motivated the evaluation. In other words, non-destructive evaluation is fundamentally about how observed manifestations of various physical principles can be utilized for improved knowledge about an object without altering its function.

For investigations linked to the evaluation of mechanical properties and geometry, stress waves provide an important framework. From a general viewpoint, stress waves in solids may be interpreted as a phenomenon similar to sound. Thus, by the analysis of the recorded sound from a structure, information can be obtained. Based on stress waves and for evaluation of concrete structures, the impact-echo (IE) method is an established and well-known technique (Sansalone and Streett, 1997). In the impact-echo method, the transient vibration from an impact by for instance a hammer or steel ball is studied. By evaluating the reverberating transient vibration response, information about the structure is gained. Whereas early studies interpreted the impact-echo method as a technique similar to ultrasonic pulse echo, more recent studies link the impact-echo method for evaluation of plate-like concrete structures to Lamb waves (Gibson and Popovics, 2005). Since Lamb waves are guided waves in elastic and isotropic plates (Auld, 1990), this means that the vibration response by a transient impact (such as that used in the impact-echo method) creates a stress wave field of very general characteristics; many structures can be approximated as plate-like, and for this reason, Lamb waves are used in a large number different applications. The main topic of this thesis concerns the application of Lamb waves for evaluation of plate-like concrete structures.

1.2 Motivation of work

The impact-echo method is today an established technique for non-destructive evaluation of plate-like concrete structures. This type of evaluation is usually limited to 1D point-wise measurements and the study of one single discrete frequency (mode). However, a transient impact creates a full wavefield with wide-band frequency containing Lamb waves, and the evaluation can thereby be extended with array based measurements to include more features (carriers of information) leading to an improved result. Literature shows a potential of such extended techniques and further developments within this subject are therefore of value.

Concrete is a heterogeneous material in which scattering and attenuation represent major challenges for ultrasonic testing. For this reason, development of techniques based on Lamb waves is important since such techniques are less influenced by scattering and attenuation due to lower operating frequency (longer wavelength). In addition, the wide band frequency content of a transient impact implies flexibility in terms of operating frequency. These two aspects are of importance in the evaluation of thick concrete structures. With the increasing demand for techniques applicable for evaluation of thick concrete structures in e.g. power plants, this serve as a motivation for this thesis and its focus on Lamb waves.

1.3 Aim, objective and limitations

The aim of this thesis is to contribute to a further development of techniques based on Lamb waves for non-destructive evaluation of plate-like concrete structures under one-sided access condition. The general scope of work is limited to material characterization of acoustic/seismic wave velocities (elastic constants) and evaluation of plate thickness; i.e. the work does *not* focus on the task of finding defects/anomalies such as cracks or delaminations.

Although the field cases in this study consider plates with thickness up to 0.5 m, the work is focused on and dedicated to be applicable also for thick (>1 m) concrete structures such as those typically used in power plant constructions; given the low (compared to ultrasonic approaches) and flexible operating frequency of Lamb waves in concrete structures, it is expected that the developments presented in this thesis are valid also for thicker (>0.5 m) plate-like concrete structures.

By first studying and investigating current existing techniques for Lamb wave evaluation of plate-like concrete structures, potential areas for further improvements are identified. With this as starting point and Lamb waves as the theoretical foundation, developments are proposed through the study of data obtained from both numerical models and practical measurements. The presented work is limited to the evaluation of plate-like concrete structures for which Lamb waves is an applicable assumption; that is, structures such as piles are not considered. From the practical perspective, the condition of one-sided access is considered throughout the thesis. The equipment is limited to an impact hammer, an accelerometer and a data acquisition card; this limitation is intentionally selected to ensure the development of techniques that is realizable with a simple and portable measurement equipment. Only a few field cases are considered in the practical measurements; naturally, for further developments it is important to study the applicability of the presented techniques and results at more field cases.

1.4 Contributions of thesis

Paper I provides a study of the reliability of estimated plate thickness from the conventional impact-echo method and a combined impact-echo and surface wave technique (Lamb wave evaluation); this study identifies a systematic error. Based on these findings, a new approach for estimation of Poisson's ratio is proposed in Paper II; this approach also highlights the potential of using multicomponent measurements. A benefit of this new approach is that a through-thickness representative estimate of Poisson's ratio is obtained. In Paper III, the analysis of Lamb waves is extended to 2D arrays, thus allowing mapping (imaging) of potential material or thickness variation in the lateral plane of the plate. In the theoretical study given in Paper IV, results that contribute to improved understanding of zero-group velocity modes in plates with material variation transversally through the thickness is presented.

1.5 Thesis outline

A literature review is given in Chapter 2. Some short notes on elastic wave theory, modelling and measurements are given in Chapter 3, 4 and 5, respectively. Results are presented in Chapter 6. Summarizing conclusions and recommendations for further work based on the experiences gained during the work with this thesis are given in Chapter 7 and 8, respectively. The bibliography containing the references in the thesis is presented in Chapter 9 and the papers are included in the Appendices

Chapter 2

Related research

2.1 General note

This chapter provides a literature review about non-destructive evaluation techniques based on elastic waves. Given the limitations of this thesis, the presentation is focused on evaluation of plate-like concrete structures under one-sided access condition. That is, although some techniques are applicable for other structural shapes as well (e.g. beams and columns), the focus is intentionally directed towards the techniques operating in plate-like applications.

2.2 Ultrasonic techniques

Techniques based on ultrasonic wave propagation can be used for non-destructive evaluation of concrete structures. The first measurements of ultrasonic pulse velocity in laboratory specimens were reported around the 1940-1950s (Bungey et al., 2006), and practical measurements from constructions sites are starting to be reported from the 1960s (Malhotra and Carino, 2004). Typically, such measurements are based on two ultrasonic transducers operating in a pitch-catch configuration to obtain the time-of-flight for the ultrasonic pulse. After the introduction of dry-point transducer (Shevaldykin et al., 2002), developments of reflection imaging techniques by means of ultrasonic echo and synthetic apertures can be noticed (Schickert et al., 2003). Such techniques are used for the creation of a reflection image in which internal objects and anomalies, such as defects, appear as points or regions with deviating colour. Consequently, techniques based on ultrasonics, and synthetic apertures in particular, are now popular for testing of concrete structures with recent developments illustrated by wireless transducer systems (Wiggenhauser et al., 2016) for large concrete structures and advanced post-processing algorithms (Müller et al., 2012) adopted from the field of geophysics. However, since concrete is a composite material of cement and aggregates, wave scattering represents a significant challenge that may restrict the possibilities for evaluation. Furthermore, high attenuation of the ultrasonic pulse do also represent a major challenge. As a result, scattering and attenuation may ultimately lead to a case in which the creation of a reflection image with desired resolution and coverage is no longer realizable (Almansouri et al., 2017). For high frequencies or large concrete structures that also may include vast amount of reinforcement bars and potentially coarse aggregates, this may be a particular problem since the amount of attenuation and scattering is related to the number of wavelengths along the propagation path of the ultrasonic pulse.

2.3 Impact-echo method

An alternative methodology, less influenced by scattering and attenuation, is to use elastic waves in a lower frequency regime compared to ultrasonics; i.e. to use a longer spatial wavelength. Naturally, compared to ultrasonic imaging techniques, this implies a decreased spatial resolution. However, on the other hand, this decreased resolution also implies a corresponding increase in the range of coverage. For evaluation of plate-like concrete structures with elastic waves operating in a lower frequency regime compared to ultrasonic approaches, the impact-echo (IE) method is a common and established technique (Sansalone and Streett, 1997; Sansalone, 1997). The method is also standardized by according to ASTM C 1383. The impact-echo method is based on the measurement of the dynamic response of the tested structure subjected to a transient impact. Ideally, this response contains a distinct frequency peak corresponding to a dominating reverberating resonant mode; the frequency of this mode is dependent on the material properties and geometry. In other words, the procedure of the impact-echo measurement corresponds to a general resonance evaluation. In its most simple form, the evaluation with the impact-echo method is based on monitoring the relative variation of the frequency response for the resonant mode at different locations of the tested structures. A variation in frequency serves as an indicator of varying material properties; faults and anomalies can thereby be detected. Examples of improvements supporting such evaluations are automatic data acquisition (Schubert and Köhler, 2008) as well as air-coupled transient source generation (Dai et al., 2013) and detection (Zhu and Popovics, 2007). Such developments facilitate the creation of an image showing the relative variation of the response along a surface (Schubert and Köhler, 2008; Zhu and Popovics, 2007).

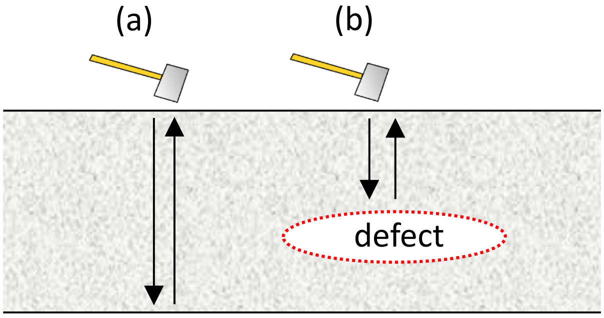

Figure 2.1: Principle of the traditional and empirical conceptual model for impact-echo testing. Figure created after Schubert and Köhler (2008). (a) Homogeneous case without anomaly. (b) Non-homogeneous case due to a flaw: a change in "travel time" and thus frequency is observed.

In the impact-echo literature, the method is traditionally explained with an empirical conceptual model (Sansalone and Streett, 1997) which is illustrated in Figure 2.1. Figure 2.1 shows the travelling path of a mechanical wave generated by an impact at the top surface. If the plate contains no flaw (Figure 2.1(a)), the wave will reverberate and create a resonance between the top and bottom plate surface. If a flaw such as a delamination is present (Figure 2.1(b)), the travel path changes, which in turn also changes the frequency of the resonance. The frequency of the resonance is for this empirical conceptual model suggested to be governed by the expression

$$F = \frac{\beta V_P}{2h} \tag{2.1}$$

with the longitudinal wave velocity V_P, the *effective* plate thickness h and the geometrical correctional factor β. Eq. 2.1 provides an estimate of the thickness h for the studied object once F, β, and V_P are known. Typically, β is assumed depending of the object geometry and for concrete plates the value is usually suggested to be equal to 0.96 (Sansalone, 1997). Early studies using the impact-echo method and this equation for estimation of thickness report accuracies within 3 % (Sansalone and Streett, 1997). However, studies with more significant deviations exist (Popovics et al., 2006, 2008; Maser, 2003). In these studies the plate thickness is underestimated in 18 of 19 locations with a mean error of -8 %. Traditionally, such deviation in results has been explained to be associated with an improper selection of value for the β factor.

As may be noticed, the empirical conceptual model of impact-echo is very similar to the model used to described ultrasonic pulse echo measurements.

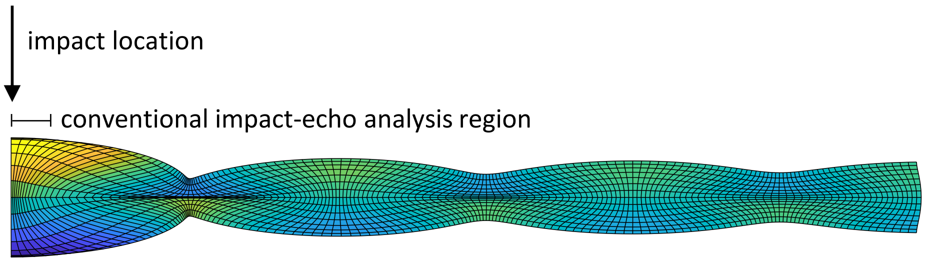

Figure 2.2: Illustration of the first symmetric (S1) zero-group velocity (ZGV) mode corresponding to the resonance mode used in impact-echo measurements on plates. Figure created after Gibson and Popovics (2005). Note the difference in spatial distribution of the mode compared to the empirical conceptual model defined by "ray paths" in Figure 2.1.

However, since the resonance mode used in impact-echo testing of plates is linked to the zero-group velocity (ZGV) point of the first symmetric Lamb mode (S1) (Gibson and Popovics, 2005), this empirical interpretation is somewhat ambiguous. This is further evident by Figure 2.2, which shows the mode shape of the S1-ZGV mode, i.e. the mode shape corresponding to resonance mode employed in impact-echo testing of plates; a major difference between the spatial distribution of this mode shape and the ray pattern (Figure 2.1) given by the classical empirical conceptual model is obvious. As explained and practically demonstrated by Abraham et al. (2011) on a plate with varying amount of reinforcement as well as tendon ducts with varying amount and type of filling, this means that the impact-echo method should be interpreted as a measurement of a resonance frequency which is dependent on the local stiffness of the plate.

Gibson and Popovics (2005) also demonstrate that the theoretically exact β factor is a function of Poisson's ratio. Although not explicitly stated, the results from Gibson and Popovics (2005) implies that for a proper evaluation of the plate properties such as the thickness parameter, Lamb wave theory must be used. In Lamb wave theory, a laterally infinite plate is defined by three independent parameters: the shear wave speed V_S, Poisson's ratio ν and thickness h (Auld, 1990). As a result, the exact thickness h of an unknown plate can only be determined with Eq. 2.1 if the longitudinal wave velocity V_P and Poisson's ration ν are known. Even though the Lamb wave interpretation of impact-echo nowadays is widely accepted, it is still not unusual to encounter the empirical conceptual model (see e.g. (Liu et al., 2017; Garbacz et al., 2017) in recent (2017) published papers. Thus, the misconception stating that the impact-echo method represents an evaluation technique with discrete and pointwise sensitivity (see Figure 2.1) rather than an evaluation technique influenced by a major volume (see Figure 2.2) may unfortunately still exist in some cases.

From a general perspective, the link between the impact-echo method and Lamb waves means that the resonance mode ideally should be interpreted as a zero-group velocity (ZGV) Lamb mode rather than a particular mode only limited to concrete plates. In fact, ZGV Lamb modes represent a general wave phenomena (Kausel, 2012; Prada et al., 2008) with some interesting applications given by: evaluation of acoustic bulk wave velocities and Poisson's ratio in metal plates with laser-based measurements (Clorennec et al., 2007), thin-layer thickness (Cès et al., 2011), hollow cylinders (Cès et al., 2012), interfacial bond stiffness (Mezil et al., 2015), and potentially air-coupled measurements (Holland and Chimenti, 2003; Zhu and Popovics, 2007).

2.4 Impact-echo and surface waves

With Lamb wave theory as base combined with the important link provided by Gibson and Popovics (2005), an extension of the basic impact-echo measurement is well motivated and sensible. Since an impact-echo measurement, which corresponds to a very general transient excitation, creates elastic waves with a wide frequency bandwidth, a natural extension is to combine the impact-echo frequency estimate (i.e. the estimate of the S1-ZGV Lamb mode frequency) with a measurement of propagating surface waves. Examples of such combined techniques are given by Kim et al. (2006); Ryden and Park (2006); Barnes and Trottier (2009); Shokouhi (2009) and Popovics et al. (2008). Although variations exist between these techniques, the main idea is still the same: by use of relations that govern wave propagation and Lamb wave theory, the Lamb wave plate parameters shear wave velocity V_S, Poisson's ratio ν and thickness h are obtained. Compared to the traditional impact-echo method, these techniques allow the estimation of the Lamb wave plate parameters (V_S, ν and h) under one-sided access test condition without the requirement of calibration cores or assumed β values. However, this comes to the price of that they all are dependent on at least three independent input quantities in order to allow the determination of the Lamb wave plate parameters; i.e. three pieces of information are required to solve a system of three variables. Naturally, there exist different approaches for how these three parameters can be obtained; this represent the topic of the following section.

2.5 Obtaining the Lamb wave plate parameters

As mentioned previously, three independent parameters define an isotropic and laterally infinite plate in Lamb wave theory: shear wave speed V_S, Poisson's ratio ν and thickness h (Auld, 1990). That is, to characterize a plate in a non-destructive evaluation based on Lamb wave theory, at least three quantities must be measured. This section will discuss and present some different ideas and techniques which can be used to solve this non-destructive evaluation task of obtaining the Lamb wave plate parameters.

Poisson's ratio

Poisson's ratio can be determined by measuring the longitudinal wave velocity and the Rayleigh wave velocity (Wu et al., 1995): the ratio between these two velocities is only dependent on Poisson's ratio. This technique is analogue to the technique in which Poisson's ratio is determined from the ratio between the longitudinal wave velocity and shear wave velocity (Auld, 1990). It is clear that for a reliable estimation of Poisson's ratio from such techniques, accurately estimated wave velocities are necessary. Furthermore, another aspect to consider is that for a representative estimation of Poisson's ratio, the two velocities should ideally be measured over the same material volume; this may impose a challenge when two wave modes of potentially different frequency (wavelength) and mode shape (sensed volume) is utilized.

Poisson's ratio can also be estimated from the ratio between the frequencies of the S1-ZGV Lamb mode and the A2-ZGV Lamb mode (Clorennec et al., 2007); the A2-ZGV Lamb mode corresponds to the ZGV point of the second anti-symmetric (A2) Lamb mode. This approach is demonstrated successfully for several thin homogenous metal plates (Clorennec et al., 2007), but only a few measurements are reported for concrete plates (Gibson, 2004; Baggens and Ryden, 2015b). The ratio between the S1-ZGV Lamb mode frequency and the Rayleigh wave velocity can also be used to determine Poisson's ratio, but this approach is limited by the requirement of a known plate thickness (Medina and Bayón, 2010).

Alternatively the amplitude ratio between the surface in-plane and surface normal components of the Rayleigh wave can be used to estimate Poisson's ratio (Bayon et al., 2005). This amplitude ratio may be interpreted as the amplitude polarization of the mode. However, to the author's best knowledge, this approach has not been demonstrated on concrete plates. Inspired by this approach, Baggens and Ryden (2015d) (Paper II) proposed and demonstrated that the amplitude polarization of the S1-ZGV Lamb mode can be used for estimation of Poisson's ratio. Compared to approaches based on data from multiple modes such as the longitudinal wave and the

Rayleigh wave, this approach provides a through-thickness representative value for Poisson's ratio since the S1-ZGV Lamb mode is present through the entire thickness of the plate.

Longitudinal wave velocity

The longitudinal wave velocity is usually estimated from the time taken by the first arriving wave from a transient impact to travel between two or multiple points separated by a known distance along the surface. A possible source of uncertainty in this type of analysis is the identification of a correct first arrival time. Unfortunately, identifying an accurate time point for the first arriving wave is not a trivial task; typically, the displacement magnitude of the first arriving wave is very small. Despite this challenge of finding the first arriving wave, a commonly used procedure is to identify the first value above a certain threshold, and assume that this observed wave corresponds to a pure longitudinal wave. An alternative approach, which may facilitate the identification of the first arriving wave, is to study the trend of the measured signal instead of using a threshold level (Popovics et al., 1998).

Additional uncertainty in measurements of the longitudinal wave velocity may occur if the material properties vary through the thickness. In such cases, the measured longitudinal wave velocity along the surface will be different from the longitudinal wave velocity measured through the plate. That is, a measurement along the surface will not provide a through-thickness representative estimation, which in turn may lead to uncertainties in the evaluation of the Lamb wave plate parameters. Gibson (2004) observed a systematic variation of this kind in which an increased velocity was observed in measurements through the thickness of the plate compared with velocities obtained from measurements along the surface. To account for such variations in velocity, Popovics et al. (2006) proposed a correction factor to compensate for the slower longitudinal wave velocity along the surface.

As an indirect alternative to a measurement based on the first arriving wave, the longitudinal wave velocity may be calculated from the Rayleigh wave velocity (Kim et al., 2006). However, this approach is dependent on the assumption of an already known value of Poisson's ratio.

Rayleigh wave velocity

A simple technique for estimation of the Rayleigh wave velocity is to study the cross correlation of two signals separated by a known distance (Wu et al., 1995). However, this technique may suffer from dispersion effects (Shin et al., 2007), and for this reason, the use of a continuous wavelet transform has been proposed. Another proposed approach for estimation of a Rayleigh wave velocity is the spectral analysis of surface waves method, SASW (Heisey et al., 1982). More recent approaches based on multichannel datsets (Ryden and Park, 2006; Barnes and Trottier, 2009) propose that the Rayleigh wave velocity can be estimated from the asymptotic trend of the fundamental Lamb modes in frequency-phase velocity domain (Park et al., 1999). Such analysis is sometimes referred to as multichannel analysis of surface waves (MASW) and is usually based on Fourier transforms in both time and space domain (Alleyne and Cawley, 1991).

S1-ZGV Lamb mode frequency

Robust estimation of the S1-ZGV Lamb mode frequency is important to ensure reliability in evaluated Lamb wave plate parameters. In Lamb wave theory, plates are characterized by laterally infinite dimensions (Auld, 1990). Naturally, this condition is rarely found in practical testing of concrete plates. Nevertheless, ZGV Lamb modes are still defined also for bounded plates (Cees et al., 2011), but reflections from surface waves and other structural modes may impose additional complexity to the interpretation of the measured frequency spectrum. Thus, to assist the identification of a correct S1-ZGV Lamb mode frequencey, time frequency analysis has been proposed (Abraham et al., 2000; Algernon and Wiggenhauser, 2007).

For the cases of combined impact-echo and surface wave measurements (e.g. MASW), the spatial distribution of the S1-ZGV mode shape may also be employed for improved detectability of frequency. For instance, by summation of the signals in vicinity to the impact source, the identification of the S1-ZGV Lamb mode frequency can be facilitated (Ryden and Park, 2006; Ryden, 2016). Another similar approach is based on a multiplication of amplitude spectrums from signals measured close to the impact source (Medina and Garrido, 2007). For both these approaches, the influence from propagating waves and scattering is reduced since the summation and multiplication amplifies the frequency of the S1-ZGV Lamb mode due to its spatially coherent characteristic.

2.6 Uncertainties and challenges

Empirical conceptual model

Although several improvements have been proposed for the impact-echo method, among them the very important link to Lamb wave theory by Gibson and Popovics (2005), it can be observed that the empirical conceptual

Test location		Estimated thickness (mm) and relative error (%)			
No	Thickness (mm)	Impact-echo (ASTM C1383)		Impact-echo and surface wave analysis (Lamb wave analysis)	
1	256	-		252	(-2%)
2	263	-		244	(-7%)
3	246	243	(-1%)	242	(-2%)
4	261	195	(-25%)	237	(-9%)
5	337	293	(-13%)	309	(-8%)
6	281	268	(-5%)	254	(-10%)
7	239	224	(-6%)	223	(-7%)

Table 2.1: Estimated thickness from impact-echo and combined impact-echo and surface wave analysis (MASW). Table created from data presented by Popovics et al. (2008).

model still is used as theoretical framework in some cases; this may be one reason to that the impact-echo method is sometimes compared and discussed as a member within the family of ultrasonic pulse echo techniques. To the author's opinion, this is somewhat sad since this interpretation may prevent the evaluation from taking full advantage of the possible information available in the excited Lamb wave field. Furthermore, and also to the author's opinion, this interpretation may also contribute to confusion in discussions about sensitivity for defects and the capability of detecting reinforcement bars etc.

Underestimated plate thickness

In the literature, a systematic error in terms of underestimated plate thickness from impact-echo measurements are observed, see Section 2.3 and Table 2.1. As example, in the results presented in Table 2.1, a systematic error is also observed for the combined impact-echo and surface wave analysis (MASW/Lamb wave analysis/right column). Baggens and Ryden (2015a) (Paper I) reproduced this systematic error in numerical simulations and also observed the error in a practical measurement with both a multichannel analysis of surface waves (MASW) and a conventional impact-echo set-up. A possible source to this systematic error is near-field effects caused by cylindrical spreading of waves from a point source and interference of localized wave modes created due to the point source excitation. Within the field of geophysics, near-field effects are observed and studied for half-spaces (Zywicki and Rix, 2005; Roesset et al., 1990; Roesset, 1998; Bodet et al., 2009). However, for the case of non-destructive testing of plates, only a few studies have recognized the influence from the near-field of a point source (Ditri et al., 1994). In the context of impact-echo thickness testing of plates, near-field effects have traditionally not been taken into account (Baggens and Ryden, 2015a) (Paper I). Baggens and Ryden (2015a) (Paper I) demonstrated that the longitudinal wave velocity estimated from the first arriving wave represent the main cause of the underestimated thickness. By instead using alternative approaches for estimation of Poisson's ratio that are independent on the longitudinal wave velocity estimated from first arrivals, this systematic error may be reduced (Baggens and Ryden, 2015d) (Paper II).

Evaluation domain

In the conventional impact-echo method, the data is interpreted and evaluated at a pointwise level. As mentioned in Section 2.3, by repeating this evaluation at multiple locations, either through an automated or manual process, variations in the response can be investigated. However, since a transient impact source is used that creates a full wave field propagating outwards from the source location, the pointwise evaluation is somewhat limited. A step in the direction of extending the evaluation domain and incorporating more information carriers within the full wave field is taken by the combined techniques described in Section 2.4. Yet, these combined techniques are typically limited to evaluation domains such as lines. With inspiration from near-surface geophysical applications (Boiero et al., 2012) and testing of metal plates (Harley and Moura, 2013), a natural extension of testing of plate-like concrete structures is to consider data collected and evaluated from a two-dimensional surface. An example of such evaluation applicable for concrete applications is demonstrated and proposed in Paper III. Compared to the impact-echo method evaluated at multiple discrete points, this approach enables the possibility to study the variation of *propagating* waves over a wide frequency bandwidth for a two-dimensional surface.

Imaging

For non-destructive imaging analysis of concrete structures with elastic waves, techniques based on ultrasonic pulse echo and synthetic apertures represent a predominant group (Pla-Rucki and Eberhard, 1995; Schickert et al., 2003; Wiggenhauser et al., 2016; Schickert and Krause, 2010). Within this field, some recent developments include application of data processing algorithms initially proposed in the field of geophysics (Müller et al., 2012; Grohmann et al., 2016, 2017). Although some ultrasonic imaging applications report the usage of frequencies as low as 25 kHz (Grohmann et al., 2016), the common range of ultrasonic test frequency is typically 50-200 kHz (Schickert and

Krause, 2010). For frequencies below this ultrasonic domain, imaging of results from impact-echo data is proposed in the literature for both B-scans (Schubert et al., 2004) as well as C-scans (Zhu and Popovics, 2007; Ohtsu and Watanabe, 2002). Some references also reports about the possibility of utilizing synthetic apertures focusing techniques on data from impact-echo measurements to enable reflection imaging transversally through the plate (Schubert and Köhler, 2008; Ganguli et al., 2012). However, to the best of the author's knowledge, no example of technique for imaging analysis with *propagating* Lamb modes and below ultrasonic frequency applied on plate-like concrete structures exists in the literature. With aim of removing this gap, a 2D arrays technique for Lamb wave phase velocity imaging of plate-like concrete structures is proposed in Paper III.

Material gradients

For testing of plate-like concrete structures with elastic waves, a condition of isotropy based on constant material properties through the plate thickness is usually assumed (e.g. the assumption of Lamb wave propagation). However, in a number of practical studies concerning concrete structures, the case of inhomogeneity due to varying material properties is being reported Abraham et al. (2012); Boyd and Ferraro (2005); Popovics et al. (2006, 1998); Popovics (2005); Qixian and Bungey (1996); Turgut and Kucuk (2006); Hu et al. (2006). It is suggested that such material variations may be caused by uneven settlement of aggregates during casting, uneven moisture distribution, material degradation or corrosion of internal steel reinforcement Neville and Brooks (2010). To better understand the influence from potential material variation through the plate thickness in techniques based on zero-group velocity modes (such as the impact-echo method), Tofeldt and Ryden (2017) (Paper IV) investigated the behaviour of the lowest symmetric zero-group velocity mode for two plates with continuously varying acoustic bulk wave velocities. They concluded that ZGV modes, similar to the S1-ZGV mode, exist and are detected with same robustness as for the isotropic case. However, depending on the magnitude of the material variation, the evaluation of representative plate properties may in practice be challenging due to additional complexity of the wave field.

Chapter 3

Elastic wave theory

3.1 Infinite spaces

Two different type of mechanical waves can exist in a three-dimensional infinite space: the longitudinal wave and the transversal wave (Auld, 1990). These two types of waves are also referred to as P-waves and S-waves, where the capital P and S represent **p**rimary or **p**ressure and **s**econdary or shear, respectively. The longitudinal wave velocity V_L in a three-dimensional infinite space is calculated according to:

$$V_L = \sqrt{\frac{E(1-v)}{\rho(1+v)(1-2v)}} \tag{3.1}$$

where E, v, ρ are the Young's modulus, Poisson's ratio and density, respectively. The transversal wave velocity V_T in a three-dimensional infinite space is calculated according to:

$$V_T = \sqrt{\frac{E}{2\rho(1+v)}} \tag{3.2}$$

The ratio between the longitudinal wave velocity and the transversal wave velocity is only dependent of Poisson's ratio and is sometimes referred to as κ and consequently given by:

$$\kappa = \frac{V_L}{V_T} = \sqrt{\frac{2(1-v)}{1-2v}} \tag{3.3}$$

The ratio κ is an important quantity, which provides a fundamental link between the acoustic bulk wave velocities V_L and V_T. The particle movements of plane longitudinal and transversal waves are shown in Figure 3.1.

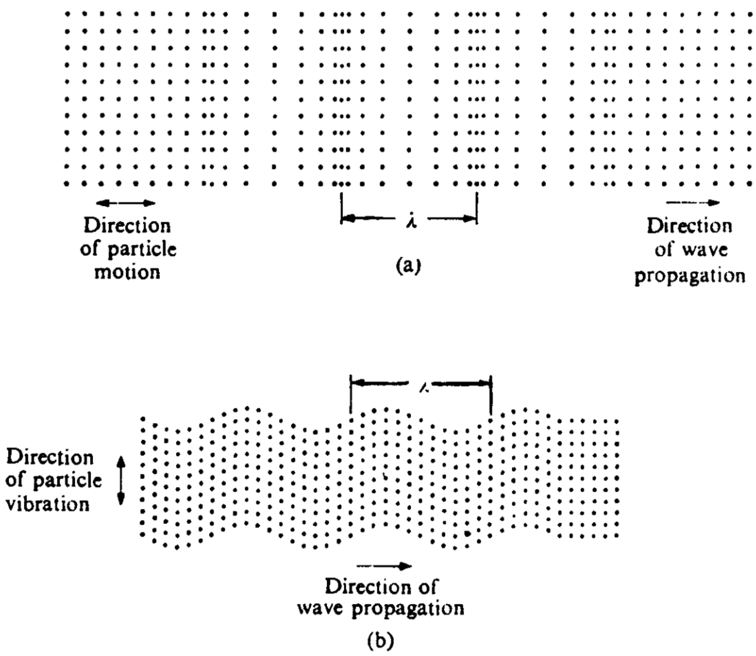

Figure 3.1: Illustration of particle motion for: (a) Longitudinal wave, (b) Transversal wave. Figure from Graff (1975).

3.2 Half-spaces

A body which is infinite below a certain plane and non-existent above this plane is typically referred to as a half-space. The probably most common example of such semi-infinite body is the earth, which is almost infinite in the lateral/horizontal direction and depth, i.e. it is only limited by the earth surface if we assume a flat earth and ignore the curvature. However, structures which are similar to half-spaces can be found in many places. Typically, it is the wavelength in comparison with the dimensions of the object that determines if an object can be assumed as infinite or not, rather than the specific dimensions of the object.

The free surface of the half-space makes it possible for surface waves to exist. Surface waves, which are often called Rayleigh waves, are created from a combination (superposition) of longitudinal and transversal waves. An example of a surface wave or Rayleigh wave is shown in Figure 3.2. Figure 3.2 shows that the displacement magnitude of the movement dominates close to the surface; hence the name surface wave.

The velocity of the Rayleigh wave cannot be determined in the same straightforward fashion as for the longitudinal and transversal wave. To determine the exact velocity, the so-called Rayleigh equation must be solved (Vik-

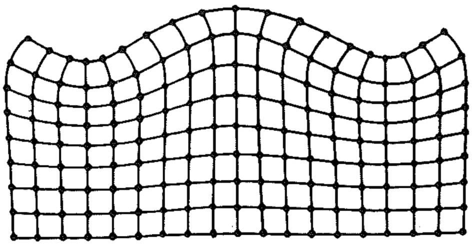

Figure 3.2: Rayleigh wave mode shape. Figure from Viktorov (1967).

torov, 1967). However, an approximation of the Rayleigh wave velocity can for example be determined from the relation given by (Achenbach, 1973):

$$\frac{V_R}{V_T} \approx \frac{0.862 + 1.14\nu}{1 + \nu} \tag{3.4}$$

3.3 Lamb waves

We have seen that two type of waves exist in an isotropic infinite body, and when a free surface exists (i.e. a half-space), Rayleigh waves can also exist. In the case of a plate, which has two free surfaces, additionally complexity is added to the wave propagation theory. This theory of wave propagation in linear elastic and laterally infinite plate is commonly referred to as Lamb wave theory.

The two free surfaces of the plate is equivalent to a traction free boundary condition, which means that the stress combined from longitudinal and transversal waves must equal zero at these surfaces. The boundary condition implicates that only certain combinations of longitudinal and transversal waves within the plate can exist at a given frequency. This means that only certain combinations of angular frequencies ω and lateral wave numbers k are possible. The valid combinations of frequencies ω and lateral wave numbers k, so-called ω-k pairs, define the dispersion characteristics of the plate, and can be obtained by solving the Lamb wave equation (Viktorov, 1967):

$$\frac{\tan(\beta h/2)}{\tan(\alpha h/2)} = -\left[\frac{4\alpha\beta k^2}{(k^2 - \beta^2)^2}\right]^{\pm 1} \tag{3.5}$$

where

$$\alpha^2 = \omega^2/V_L^2 - k^2$$
$$\beta^2 = \omega^2/V_T^2 - k^2$$

V_L and V_T are the longitudinal and transversal wave velocities, respectively, and h represents the plate thickness. The Lamb modes are divided into two

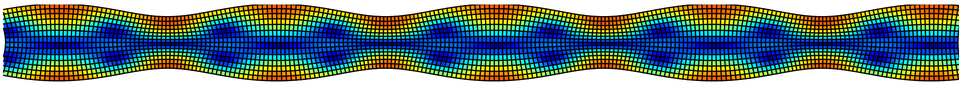

Figure 3.3: Example of symmetric Lamb mode.

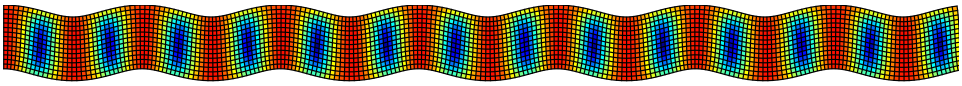

Figure 3.4: Example of anti-symmetric Lamb mode.

main families: symmetric and anti-symmetric modes. The positive sign of the exponent on the right side of Eq. (3.5) defines symmetric modes, whereas the negative sign defines anti-symmetric modes. Examples of a symmetric and an anti-symmetric Lamb mode are shown in Figure 3.3 and Figure 3.4, respectively.

The valid ω-k pairs define the dispersive characteristics of the plate. The dispersion of Lamb waves contain important information which can for example be used to determine the elastic plate properties and thickness. The dispersion relations for a plate can be illustrated in many ways. One example is to plot the ω-k pairs for each Lamb mode directly, see Figure 3.5. Another possibility is to present the dispersion curves in the frequency-phase velocity domain, see Figure 3.6. The Rayleigh wave velocity can, for example, be determined by studying the convergence of the phase velocities for the A0 and the S0 modes, see Figure 3.6. The S1-ZGV point, which is the point of the minimum frequency of the S1-mode, is another quantity which can be determined. The frequency of this point corresponds to the reverberating resonance used in traditional impact-echo measurements (Gibson and Popovics, 2005).

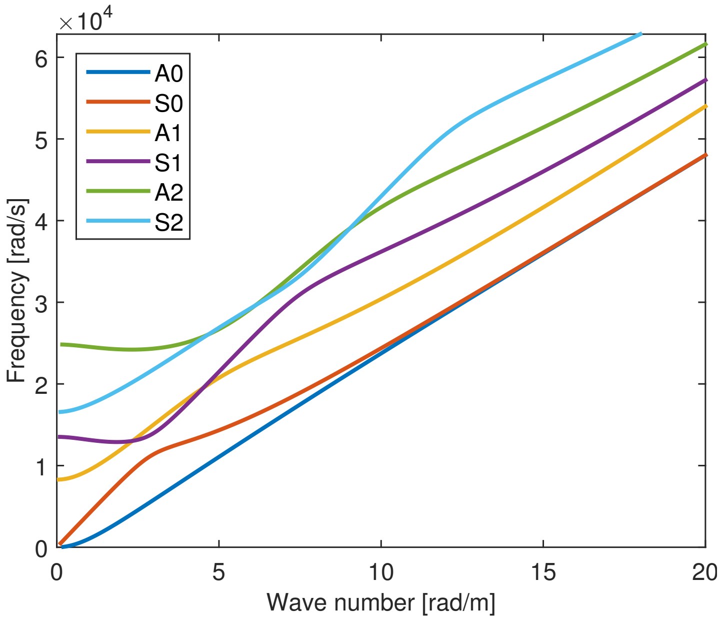

Figure 3.5: Dispersion curves (wave number-frequency plot) for a plate with Young's modulus 40 GPa, Poisson's ratio 0.2, density 2400 kg/m^3, and thickness 1 m.

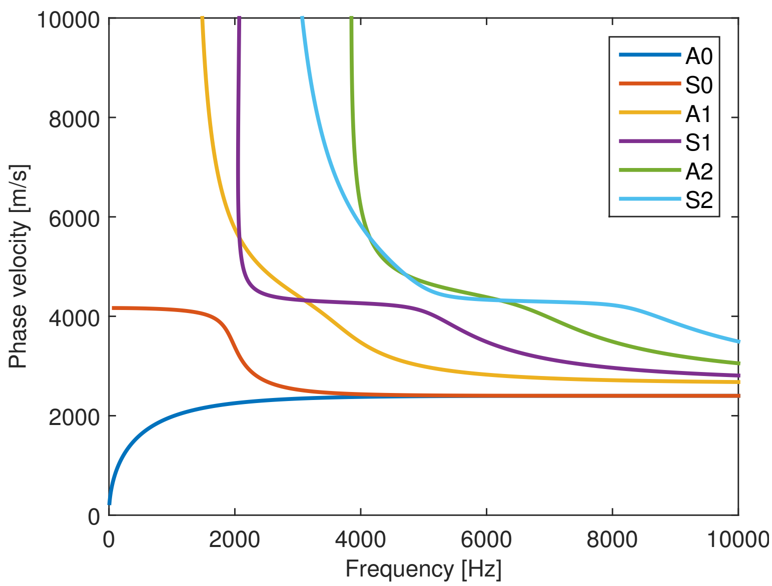

Figure 3.6: Dispersion curves (frequency-phase velocity plot) for a plate with Young's modulus 40 GPa, Poisson's ratio 0.2, density 2400 kg/m^3, and thickness 1 m.

Chapter 4

Numerical modelling

4.1 Calculation of dispersion curves

Although Eq. 3.5 is written in a compact and explicit form, the solution of this equation is not trivial, and must typically be performed with numerical approaches. For the cases of plate with continuous material variations, as in Paper IV, no simple and closed form expression as Eq. 3.5 exists. As approach for handling these cases, a semi-analytical finite element (SAFE) technique is adopted in Paper IV. This approach is based on the methodology presented by (Predoi et al., 2007; Bartoli et al., 2006; Treyssède and Laguerre, 2013) and implemented in the commercial FE code COMSOL (COMSOL Inc., 2016) and MATLAB.

4.2 Response due to point source excitation

The finite element software COMSOL (COMSOL Inc., 2016) and the computational software MATLAB are used to perform simulations of wave propagation in elastic plates. The following presentation will focus on the implementation of a finite element model which simulates the response of a plate subjected to transient impacts. This implementation is mainly based on the modelling techniques presented by Castaings et al. (2004); Hosten and Castaings (2006); Ryden and Castaings (2009). This approach for modelling is selected since it allows control over the mesh size and the absorbing region. Since the computation is performed in frequency domain, an uncoupled problem is obtained; this problem can efficiently be solved in parallel thus allowing a potential speed-up.

As an example model in this presentation, an axially symmetric plate model

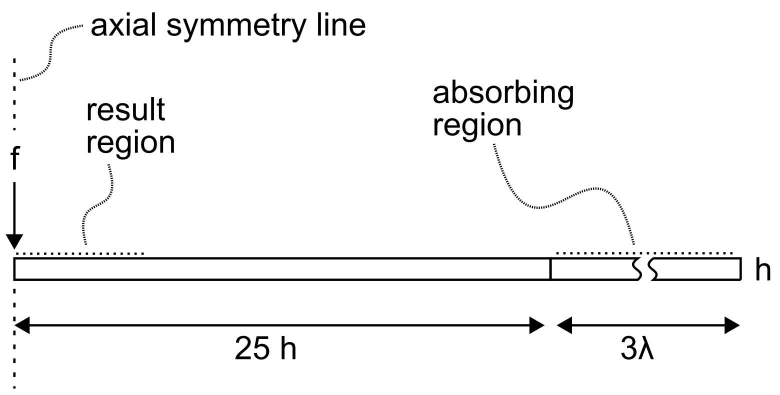

Figure 4.1: Sketch of plate model.

is shown in Figure 4.1. This type of model corresponds to the model type used in Paper I, Paper II and Paper IV. A load is applied at the axial symmetry axis to simulate the point load. The plate is divided into two main regions: result region and absorbing region. The response is extracted from the result region whereas the absorbing region is used to simulate infinite boundaries of the plate. The absorbing region is created by a gradually (cubically) increasing damping ratio (Castaings et al., 2004; Ke et al., 2009).

The model is solved in frequency domain using an element mesh and absorbing region which are adjusted to the frequency. At low frequencies a coarse mesh is used, as opposed to the case of high frequencies where a fine mesh is used (Ryden and Castaings, 2009). The absorbing region is adjusted according to frequency; a longer absorbing region is used for low frequencies and the opposite. The response of the plate in terms of complex amplitudes, i.e. the so-called frequency response function, is extracted from the result region of the plate, see Figure 4.1. The absolute amplitude of an example frequency response function is plotted in Figure 4.2.

Force excitation pulses, are applied at the axial symmetric axis to simulate a point load (see Figure 4.1). These pulses are defined using a Gaussian monopulse. An example of a force excitation pulse is shown in Figure 4.3. The dynamic response to the point load excitation in time domain are obtained from the inverse discrete Fourier transforms of the frequency response functions multiplied with the frequency spectrum of the pulses (Castaings et al., 2004). An example of dataset in time domain is shown in Figure 4.4. As a graphical illustration of the modelling process, an overview of the simulation technique is shown in Figure 4.5.

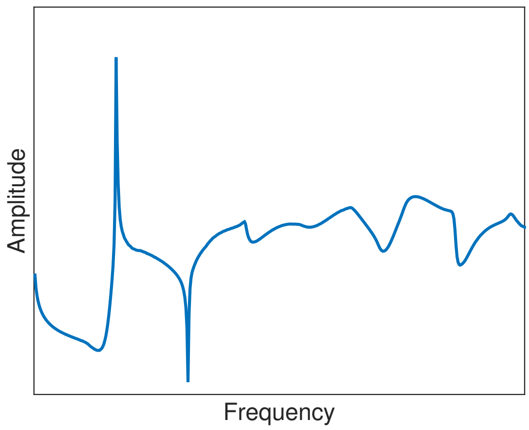

Figure 4.2: Example of the absolute value of frequency response function.

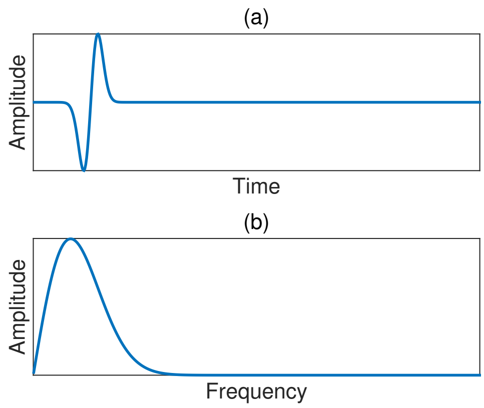

Figure 4.3: Example of force excitation pulse in (a) Time domain, (b) Frequency domain.

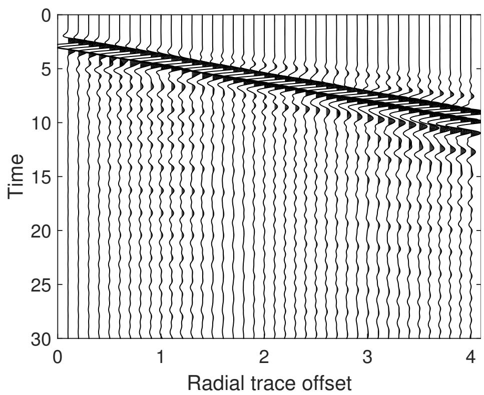

Figure 4.4: Example of dynamic response in time domain.

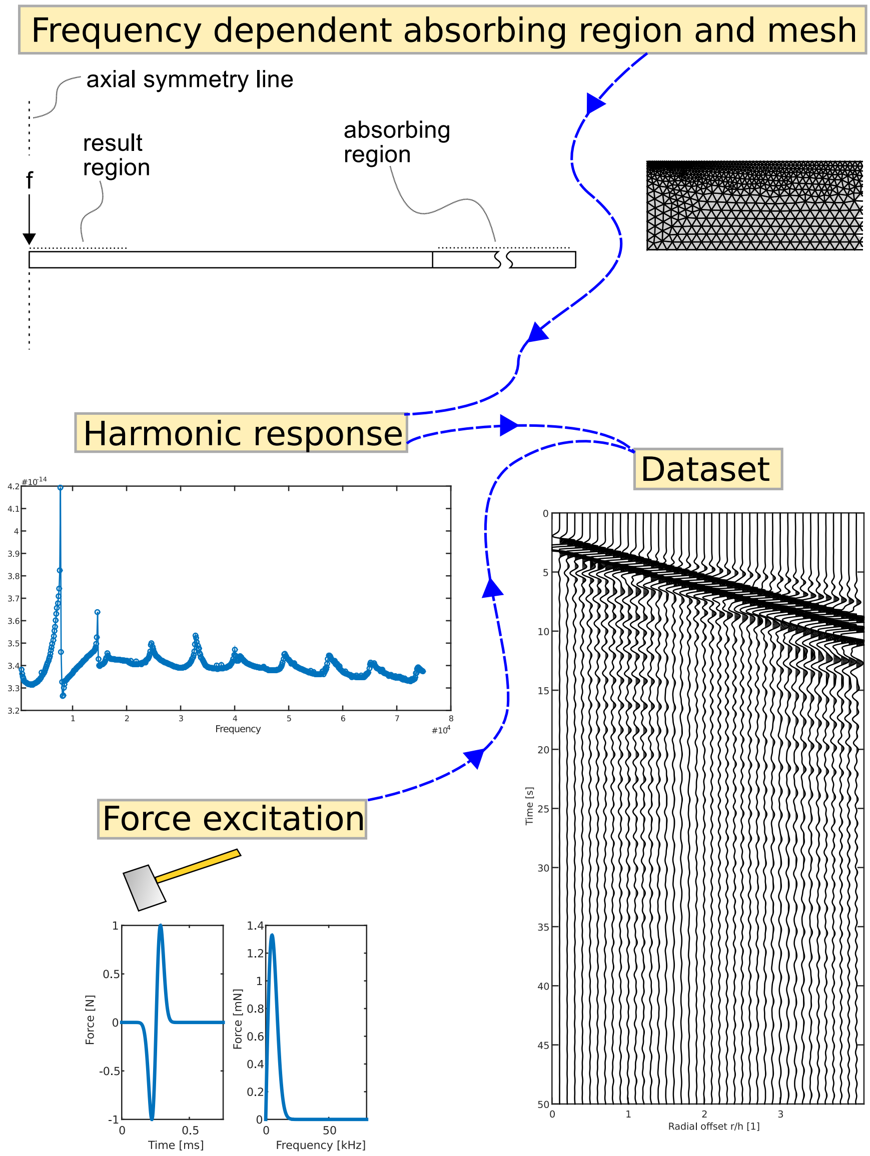

Figure 4.5: Overview of modelling technique.

Chapter 5

Measurement equipment

Practical measurements in this thesis are performed with an equipment consisting of an impact hammer as source and an accelerometer as receiver. The practical measurements are executed by performing several hammer impacts at increasing offset distance from the accelerometer which is kept at a fixed position throughout the measurement. By connecting the impact hammer and accelerometer to a data acquisition card, the structural response in terms of acceleration as well as the time history of the impact-force from the hammer is recorded. The recorded data are stored and saved in a laptop computer. Since the impact hammer also works as a triggering device, the reciprocity theorem for linear elastic system allows the creation of a time-synchronized multichannel dataset. This type of multichannel/ array based dataset is typical for a combined impact-echo and surface wave analysis, but the type of dataset is also observed in many other non-destructive applications as well as geophysical measurements. A sketch illustrating the practical measurement techniques and procedure is shown in Figure 5.1.

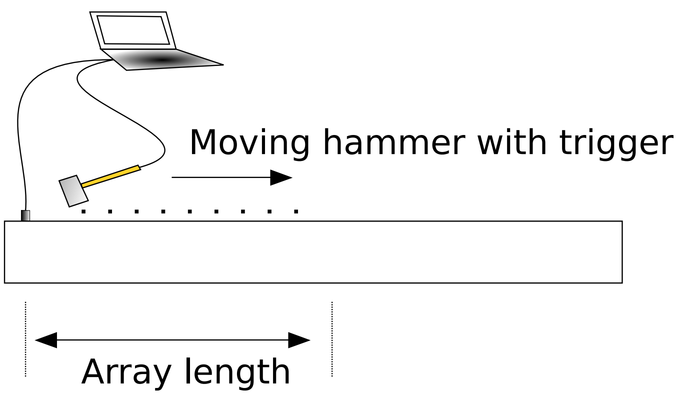

Figure 5.1: Sketch of measurement technique.

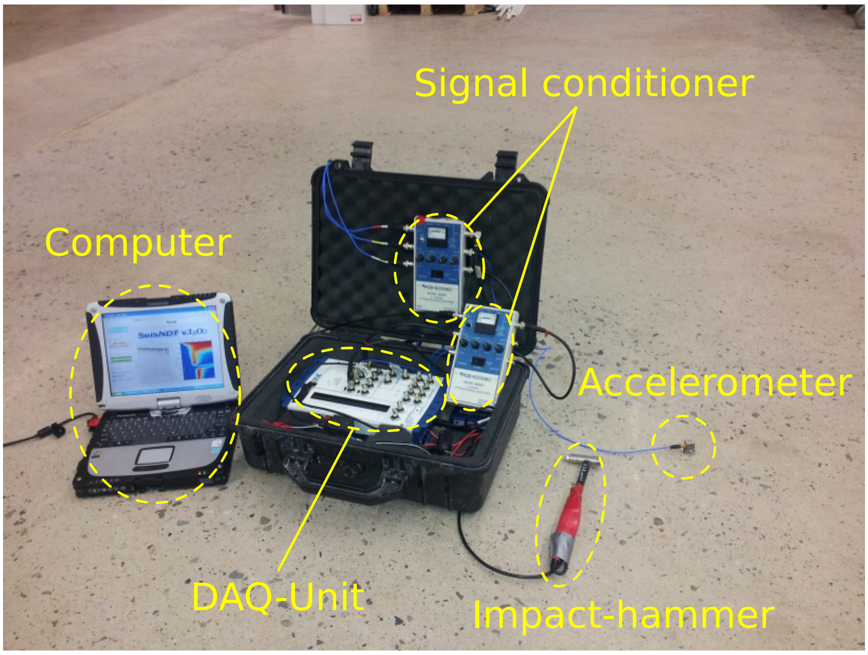

Figure 5.2: Measurement equipment: impact-hammer (PCB model 086C03), accelerometer (PCB model 339A30), signal conditioner (PCB model 480b21), DAQ-unit (NI USB-6251 BNC), and computer (Panasonic Toughbook).

An overview of the used measurement equipment is shown in Figure 5.2. Figure 5.3 shows an example of a three component accelerometer. As can be noticed, the measurement equipment represent a very portable and flexible system in which every individual part of equipment easily can be changed or replaced. For example, it is common to select impactor with respect to the object that is studied. If a thick structure is considered it is suitable to use a heavier impactor which can generate sufficient low frequencies in the impact pulse. On the contrary, if a thin structure is considered, it is suitable to use a lighter impactor which can generate sufficient high frequencies in the impact. An example of different impactors is shown in Figure 5.4.

Figure 5.3: Three component accelerometer (PCB model 339A30).

Figure 5.4: Impact hammers, from left: home-made impactor (screw/bolt) with piezoelectric crystal, hammer PCB model 086C03, hammer PCB model 086D05.

Chapter 6

Results

6.1 1D array measurements and analysis

Non-destructive techniques based on mechanical waves generated by transient impacts can be used to evaluate the thickness of plate-like concrete structures. Paper I provides increased knowledge about the reliability and uncertainties in such type of evaluations under the condition of one-sided access, i.e. the case in which only one side of the plate surface is accessible. More specifically, the investigation is focused on a combined technique based on multi-channel analysis of surface waves (MASW) and Impact-Echo (IE), see Paper I; this technique is denoted MASW/IE. In the current case, the MASW/IE technique uses the first thickness resonance of a plate (S1-ZGV) as well as the propagating surface wave field to enable a Lamb wave analysis. In addition, results are also compared with the conventional Impact-Echo (IE) method based on a simplified and interpretation of the wave behaviour, see Section 2.3.

The resonant vibration mode linked to the S1-ZGV Lamb mode as well as surface waves can be utilized to determine an unknown thickness as well as the elastic properties of a plate-like structure. Thus, Lamb wave theory plays an important role in impact-based evaluations of plate-like concrete structures and should therefore be taken into account for best possible results. In Lamb wave theory, a plate is defined by three independent parameters such as acoustic wave velocity, Poisson's ratio and thickness; in the following section and in Paper I, this represents an important basis used for non-destructive evaluation. As presented in Chapter 2, a systematic error in terms of underestimated plate thickness is reported in the literature. To study this error in more detail, the basis of the Lamb wave evaluation must be investigated; fundamentally, estimation of the elastic properties (acoustic wave velocity and Poisson's ratio) and thickness using Lamb waves is equiv-

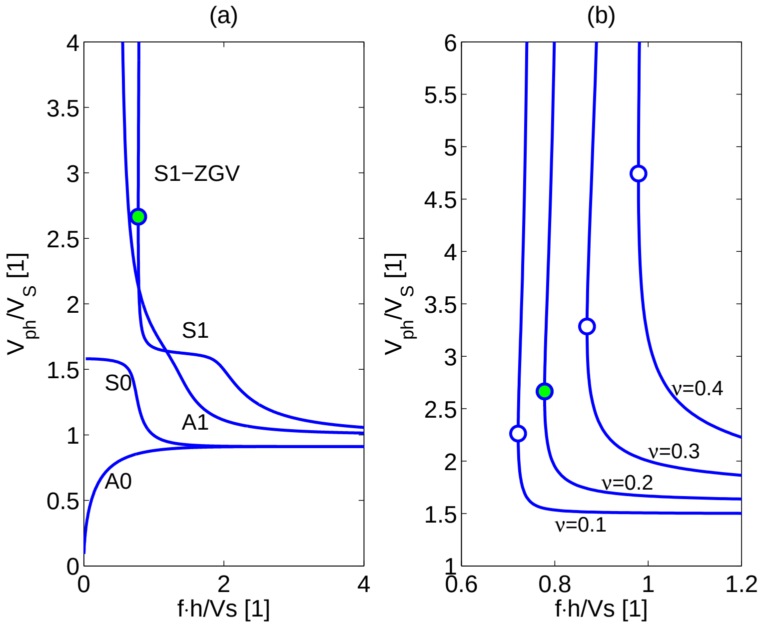

Figure 6.1: (a) Lamb wave dispersion curves (A0, S0, A1, and S1 mode) for a plate with $\nu = 0.2$. (b) Expanded view around the S1-ZGV point for different values of Poisson's ratio ν.

alent to determine the right set of Lamb wave dispersion curves associated with a plate. Here, note that since the Lamb wave plate parameters are coupled through the Lamb wave equation, the error in estimated thickness typically implies an error in an estimated elastic properties as well.

For plates in general, the dispersive nature of Lamb waves can be illustrated in many ways: one possibility is to present dispersion curves in the frequency-phase velocity domain. Here, the dispersion curves provide an important theoretical basis that facilitates the interpretation of how an unknown thickness for plate-like concrete structures can be estimated with Lamb waves. Figure 6.1 (a) shows a selection of the dispersion curves (Lamb modes A0, S0, A1, and S1) for a plate with Poisson's ratio $\nu = 0.2$. The axes are normalized with the thickness h and the transversal wave speed V_S. This normalization makes the curves only dependent on the Poisson's ratio ν, i.e. they are valid for all plates with $\nu = 0.2$. The S1-ZGV point, which represents the first through thickness resonance of a linear elastic isotropic plate, is also illustrated.

Figure 6.1 (b) shows an expanded view of the S1-ZGV point for different values of Poisson's ratio ν. Again, the normalized axes makes the location of the S1-ZGV point to be only dependent on ν. This implies that the value of fh/V_S, i.e. the normalized frequency and location on the x-axis, is constant for the S1-ZGV point at a fixed value of ν. Thus, the normalized frequency fh/V_S provides a direct way to determine the plate thickness once V_S, ν, and f are known. However, in practice, the plate parameters V_S, ν and h are in most cases not directly accessible, and as a result, they must be determined indirectly using other parameters. In the investigated MASW/IE technique in Paper I, this is solved by a measurement of the longitudinal wave velocity V_P, the Rayleigh wave velocity V_R, and the frequency of the zero-group velocity (ZGV) point of the first symmetric (S1) Lamb mode f_{S1-ZGV}. These three quantities provide the necessary information to determine V_S, ν and h, and naturally, the accuracy of the obtained parameter estimates is therefore dependent on the accuracy of these input values (V_P, V_R and f_{S1-ZGV}) in the evaluation.

A detailed numerical finite element simulation mimicking the MASW/IE and IE measurement is performed to enable an investigation of the input values in the evaluation (i.e. V_P, V_R and f_{S1-ZGV}). A description of the simulation technique is given in Section 4.2. The simulation corresponds to the calculation of the dynamic response of a plate excited with a transient point load. Results from such simulation are shown in Figure 6.2(a) which displays the time history (y-axis) of the vibration response as function of radial offset position (thickness normalized) from the point source (x-axis). For both the combined MASW/IE and conventional IE technique, the longitudinal wave velocity V_P is generally estimated from the velocity of the first arriving wave. This velocity is often referred to as the first arrival velocity. An expanded view close to the impact source, see Figure 6.2(b), reveals that there exists a zone where the velocity of the first arriving (white dots marked First arrivals) wave cannot be directly linked to the theoretical longitudinal wave velocity (solid white line marked V_P). This zone, in which the high amplitude of the Rayleigh wave hides the longitudinal wave, results in an underestimated velocity, which in turn, leads to an uncertain estimation of Poisson's ratio and an underestimated thickness. The magnitude of the underestimated thickness is dependent on Poisson's ratio, pulse frequency content, and the distance between the measurement and the impact source.

For the MASW/IE technique, the velocity of the first arrival wave is calculated by adjusting a slope to the points corresponding to first arrivals seen in Figure 6.2(b) using linear regression. For the conventional IE technique, the first arrival velocity is also calculated by adjusting a slope, but with the difference that only two signals (traces) are used; this corresponds to the procedure described by the standardization of the IE technique (ASTM C 1383). Figure 6.3(a) and Figure 6.3(b) show the variation of estimated first arrival velocity for the combined MASW/IE technique and the conventional IE technique, respectively. Both Figure 6.3(a) and Figure 6.3(b) show that the estimated first arrival velocity is clearly affected by the near field: this leads to uncertainty in the estimation of plate thickness.

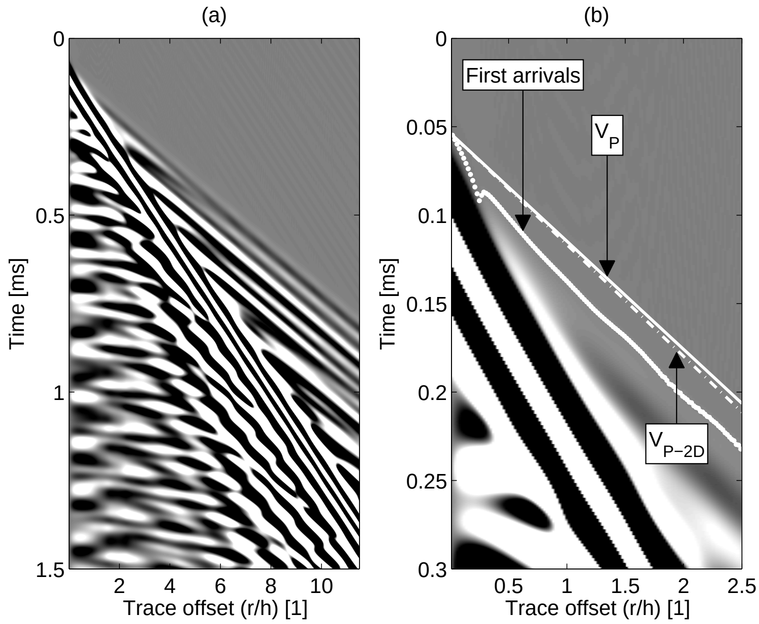

Figure 6.2: (a) Detailed finite element simulation of impact-echo and surface wave test. (b) Expanded view close to impact source showing traces/signals within a radial distance of $2.5 \cdot r/h$. First arrivals are marked with dots. Straight lines marked V_P and V_{P-2D} correspond to theoretical velocities of the longitudinal wave and low frequency component of the fundamental symmetric (S0) Lamb mode, respectively. The straight lines are aligned with the time point of the first picked arrival wave at $r/h = 0$.

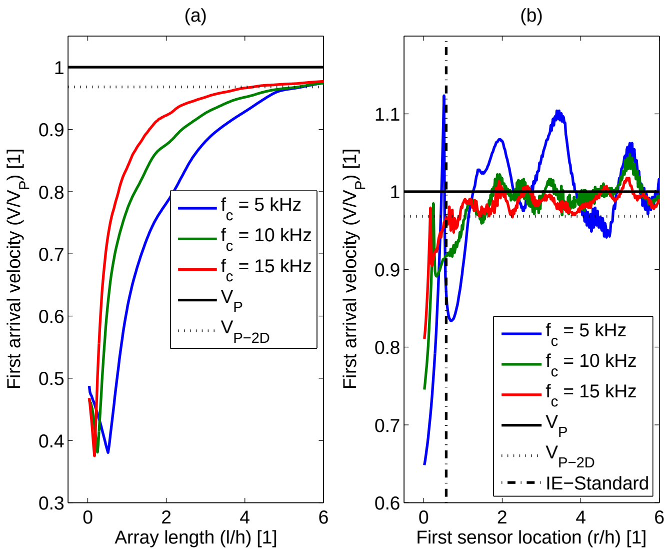

Figure 6.3: Variation of P-wave velocity estimated from first arrival in simulated data for (a) Combined MASW/IE technique (b) conventional IE technique.

To explore at which extent the observed variations in estimated first arrival velocity presented in Figure 6.3 can be observed in a real field case, an analysis of data recorded from a real measurement on a concrete cement plate cast on a granular base is performed. The variation of estimated first arrival velocity for the combined MASW/IE technique and the conventional IE technique is shown in Figure 6.4, respectively. From the results of this measurement, it can be observed that the longitudinal wave velocity estimated from the first arrivals increases with the array length (Figure 6.4(a)) or the location of the sensors (Figure 6.4(b)). This is in line with the general trend displayed by the results from the simulated case shown in Figure 6.3. Consequently, results from both simulations and measurements verify the inherently difficult and questionable task of estimating the longitudinal wave velocity V_P from the first arrivals of dispersive Lamb waves. That is, by following the recommendations in the standard ASTM C 1383 or the practice used in many applications, uncertainties in the estimated longitudinal wave velocity may arise depending on the plate properties and the impact source frequency content.

Except for the longitudinal wave velocity V_P, the Rayleigh wave velocity V_R and the frequency of the zero-group velocity (ZGV) point of the first symmetric (S1) Lamb mode f_{S1-ZGV} are also used in the evaluation of the Lamb wave plate parameters V_S, ν and h. Results from simulations and measurements show that the Rayleigh wave is also affected by near field

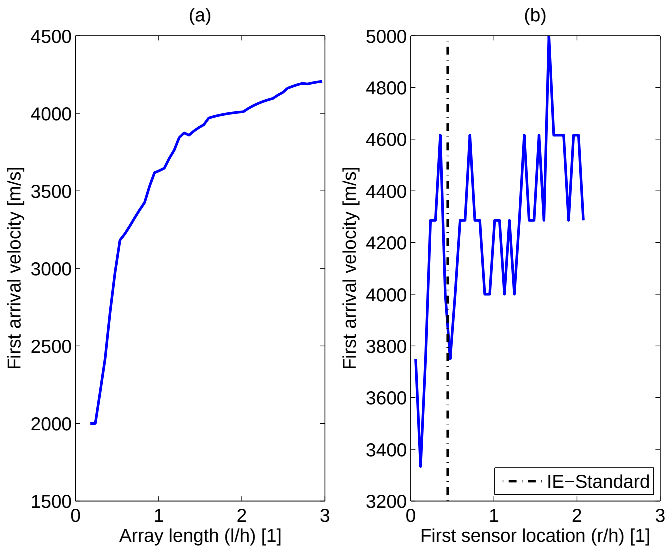

Figure 6.4: Variation of P-wave velocity estimated from first arrival in measurement data for (a) Combined MASW/IE technique (b) conventional IE technique.

effects; close to the impact source, a lower value of the estimated Rayleigh wave velocity is observed. However, the influence from this error is lower than the influence of the error from the estimation of the longitudinal wave using first arrivals. Moreover, simulations and measurements show that the S1-ZGV frequency in general is estimated with good accuracy with a non-significant dependency on the array length.

In total, the combined errors from the estimated longitudinal wave velocity and the Rayleigh wave velocity create a systematic error which underestimates the thickness in evaluations based on the MASW/IE and IE techniques with about 5-15 % depending on the Poisson's ratio, measurement set-up and source pulse. The major cause of this error is related to the interpretation of the first arrival velocity as a pure longitudinal wave velocity. Typically, for the MASW/IE technique, the underestimated longitudinal wave velocity causes an underestimated Poisson's ratio (estimated from the longitudinal wave velocity and the Rayleigh wave velocity) which in turn leads to an underestimated plate thickness. For the IE technique, the underestimated longitudinal wave velocity leads to an underestimated plate thickness through the evaluation of Eq. 2.1. Here, note that the alternative interpretation of the first arrival longitudinal wave velocity as the low frequency component of the fundamental symmetric (S0) Lamb mode (V_{P-2D} in Figure 6.2(b)) does not reduce this error.

Fortunately, the longitudinal wave velocity is not a requirement to enable

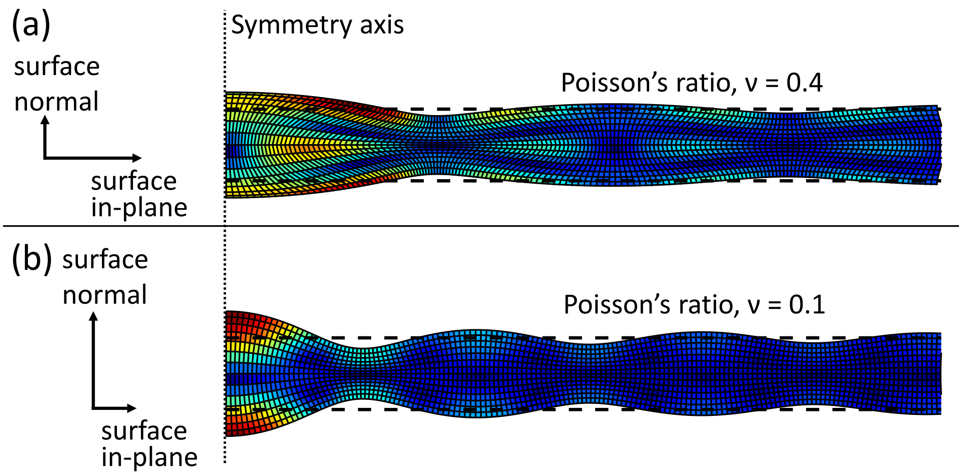

Figure 6.5: Mode shape, with cylindrical spreading due to a point load, of first symmetric zero-group velocity Lamb mode (S1-ZGV): (a) $\nu = 0.4$, (b) $\nu = 0.2$. The arrows exemplify the relative magnitude of the movement, i.e. they are not plotted in exact scale. Color scale corresponds to magnitude of displacement (i.e. both surface normal and surface in-plane component)

an estimation of the Lamb wave plate parameters (e.g. V_S, ν and h); the longitudinal wave velocity is just one alternative selection of an indirect parameter used as input in the evaluation of Poisson's ratio ν. Naturally, it is of interest to explore alternative approaches for estimation of Poisson's ratio ν which are not dependent on an evaluation of a longitudinal wave velocity from first arrival velocity. This represents the motivation for the work presented in Paper II, in which an alternative and new approach for estimation of Poisson's ratio is proposed. This approach is based on the amplitude polarization of the first symmetric zero-group velocity Lamb mode (S1-ZGV). Here, the amplitude polarization is interpreted as the ratio defined by the magnitude of the surface normal component divided by the magnitude of the surface in-plane component. This means that the approach does not require an estimation of the longitudinal wave velocity, e.g. from first arrivals as in Paper I; the longitudinal wave velocity is used to estimate Poisson's ratio together with the Rayleigh wave velocity.

The main idea of the approach is illustrated in Figure 6.5. Figure 6.5 shows the mode shape of the first symmetric zero-group velocity Lamb mode (S1-ZGV) for two values of Poisson's ratio ($\nu = 0.4$ and $\nu = 0.1$). The effect from cylindrical spreading, due to a point source excitation, is also taken into account in Figure 6.5, i.e. the spatial periodicity is defined by a Hankel function instead of an exponential function. For high Poisson's ratio, the

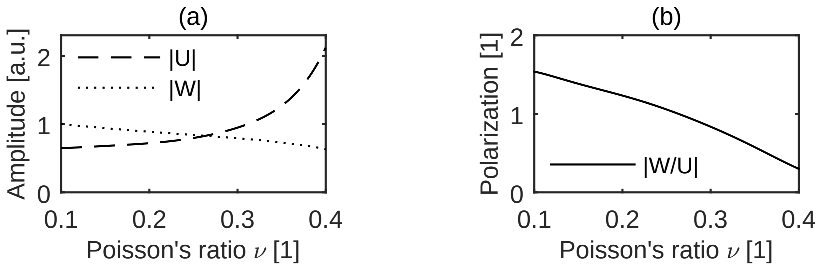

Figure 6.6: (a) Magnitude values of the surface in-plane component U and the surface normal component W of the S1-ZGV mode at the plate surface as function of Poisson's ratio ν. (b) Polarization $|U/W|$ of S1-ZGV mode as function of Poisson's ratio ν.

movement of the S1-ZGV mode shape *at the plate surface* is dominated by the surface in-plane component, see Figure 6.5 (a), whereas for low Poisson's ratio, the movement *at the plate surface* is dominated by the surface normal component, see Figure 6.5 (b). This phenomena is further illustrated in Figure 6.6(a) in which the magnitude of the surface in-plane component U and the surface normal component W is calculated for the S1-ZGV mode *at the plate surface*. The ratio defined by $|U/W|$, i.e. the amplitude polarization of the S1-ZGV mode shape, is only dependent on Poisson's ratio, see Figure 6.6(b). Once this ratio, i.e. the amplitude polarization of the S1-ZGV mode, is determined, the relationship displayed in Figure 6.6(b) provides an estimate of Poisson's ratio. In contrast to the approach based on a longitudinal wave velocity and Rayeleigh wave velocity (see Paper I), an advantage of using the polarization of the S1-ZGV Lamb mode is that a through-thickness representative estimation of Poisson's ratio is obtained, since the utilized Lamb mode (S1-ZGV) exists through the entire thickness of the plate.

The polarization based approach is tested in a practical measurement on a concrete wall in a bridge. A photograph of the bridge is shown in Figure 6.7(a). Figure 6.7(b) and Figure 6.7(c) show the test location on the wall and a close-up view of the accelerometer, respectively. Results from the evaluation of the measurement data collected from the bridge wall are shown in Figure 6.8. Figure 6.8(a) shows the absolute amplitude of the measured S1-ZGV Lamb mode (markers). A best match between the extracted mode shape (markers) and the theoretical mode shape (lines) is determined. In this case, the polarization $|W/U|$ is estimated to 1.09, and thereby, an estimate of Poisson's ratio $\nu = 0.24$ is obtained using the relationship presented in Figure 6.6(b).

In this field case, no exact value of ν is accessible directly for comparison. Nevertheless, the estimation of ν can be verified indirectly to a certain extent

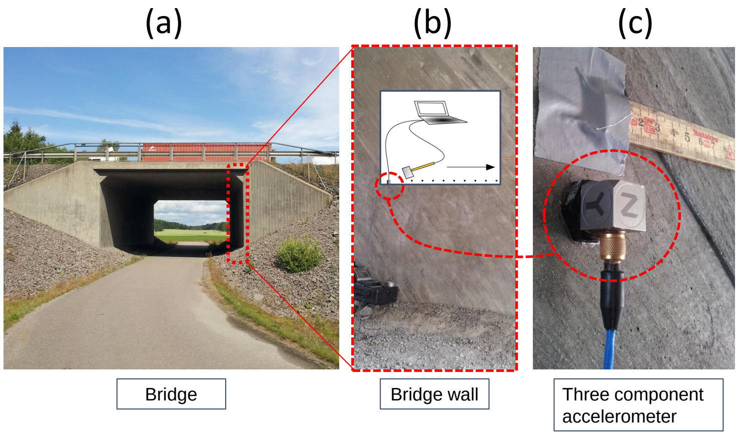

Figure 6.7: Photographs from a practical test of polarization approach. (a) Bridge test object. (b) Bridge wall. (c) Expanded view of accelerometer mounted on the bridge wall.

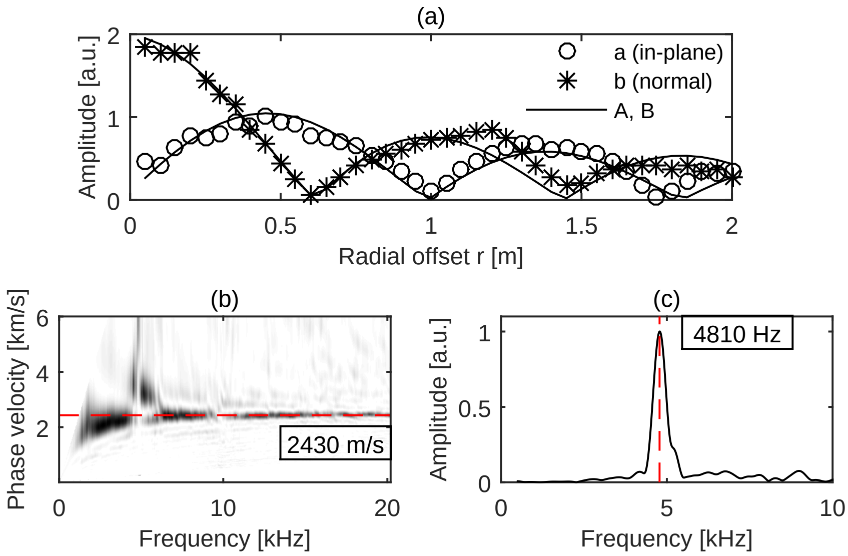

Figure 6.8: Evaluation of measurement data from practical test of the polarization approach. (a) Circle and asterisks markers: measured absolute values of the magnitude of the S1-ZGV Lamb mode. Solid lines: best fitted mode shaped to measurement data points. (b) Measurement data displayed in frequency-phase velocity domain. Red dashed line at 2340 m/s indicate estimated Rayleigh wave velocity. (c) Frequency spectrum of signal collected in vicinity of the accelerometer. Frequency peak at 4810 Hz corresponds to the S1-ZGV frequency.

from the nominal thickness of the bridge wall $h = 0.450$m. Estimation of the Rayleigh wave velocity (2430 m/s) from the raw signals displayed in frequency-phase velocity domain (Fig. 6.8(b)), the S1-ZGV frequency (4810 Hz) from the frequency spectrum of the signal nearest the impact point (Fig. 6.8(c)), and Poisson's ratio (0.24) theoretically corresponds to a thickness of 0.447 m, which is within 1% error of the nominal thickness (0.450 m). For comparison, the approach based on the longitudinal wave velocity yield an estimated thickness of 0.425 m (i.e. within 6% error of the nominal thickness). In this comparison, the same Rayleigh wave velocity (2430 m/s) and S1-ZGV frequency (4810 Hz) are used; the difference in estimated thickness between the two approaches is related to the value of Poisson's ratio $\nu = 0.18$ when the longitudinal wave velocity (4295 m/s) is estimated from first arrivals (not shown). In other words, in this field case the approach based on the polarization of the S1-ZGV Lamb mode provides an increased accuracy of the estimated nominal thickness in comparison with the traditional approach using the longitudinal wave velocity estimated from first arrivals.

6.2 2D array measurement and analysis

The work in both Paper I and Paper II is based on the study of data recorded with multiple impacts with equidistant spacing performed along a line; such data provides estimates that are representative for the region along the line. However, for improved knowledge and resolution of obtained estimates from evaluation techniques in the lateral plane of plates, it is of interest to not restrict the analyses to only a few points or a line in just one direction. However, there is no explicit requirement that prohibit the use of other layouts for data collections. For instance, layouts in form of grids are observed within the field of geophysics in studies of surface waves as well as in the general field of guided wave testing. Naturally, from the assumption of cylindrical spreading from a point source excitation, it is evident that the wave field is possible to study in all directions from the source location. This represent the motivation for the work in Paper III, in which a Lamb wave analysis technique for concrete plates with 2D-arrays is proposed. Since this technique uses data collected over a surface, a study of potential material variation and thickness along the lateral plane of the plate is possible. Compared to ultrasonic reflection imaging methods, this technique is not limited to a specific operating frequency (transducer) since it is based on a full wave field dataset with wide frequency bandwidth. Thus, the technique represent an important complement to current ultrasonic reflection imaging methods.

The 2D-array technique is demonstrated on a newly cast concrete slab that represent the ground floor and foundation in a future school. The nominal

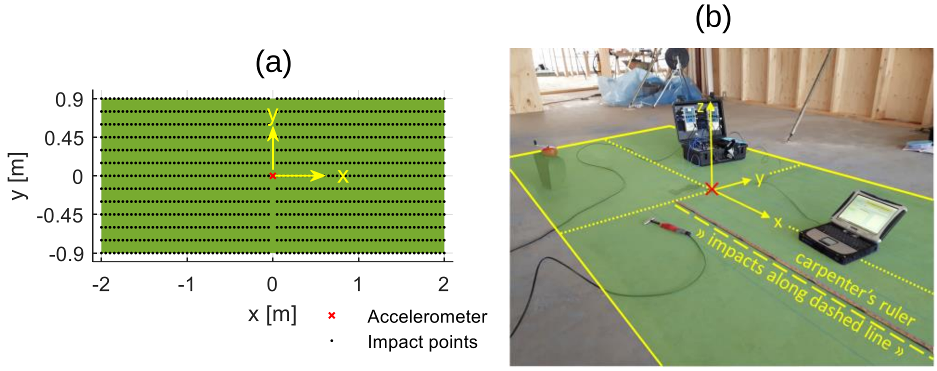

Figure 6.9: (a) Sketch of measurement domain with coordinate system. Black dots show locations of impacts and red-cross shows the location of the accelerometer, which is kept fixed throughout the measurement. (b) Photograph from measurement with illustration of surface domain in which data is collected.

thickness of the slab is 0.12 m. The measurement is carried out in a location with low influence from reflections caused by free slab edges. Also, since the plate is newly cast, a test condition without anomalies such as defects is anticipated; thus, this ideally implies uniform material properties and plate thickness. The selection of this location for the measurement is motivated with the aim of creating a controlled and reliable test environment without introducing excessive uncertainties from potential anomalies. Measurement data is collected within a rectangular domain with length 4 m and width 1.8 m, see Figure 6.9(a). Figure 6.9(a) shows the measurement domain with green colour and the associated coordinate system. Within this rectangular measurement domain, 1040 impacts are performed with locations according to the black dots. Throughout the measurement, the accelerometer is kept fixed at the centre of the rectangular domain (red cross). A photograph from the measurement is shown in Figure 6.9(b) along with illustration of the measurement domain and associated coordinate system. A practical aspect related to the measurement is also shown in Figure 6.9(b) by means of the highlighted dashed line and carpenter's ruler; the measurement is carried out by performing impacts along the dashed line, and then, moving the carpenter's ruler to a new location and repeating the process. Thus, the measurement may be interpreted as a series of measurements similar to that for instance used in multichannel analysis of surface waves (MASW, see Paper I). In the measurement, the impact hammer also works as a triggering device. As a result, reciprocity can be used to create a dataset corresponding to a full wave field recorded with 1040 time-synchronized *synthetic* sensors located at the position of the impact points. Then, by creating subset of these 1040 sensors through smaller groups, spatial sensor arrays are created. Here, focus are directed to group of sensors extracted from limited two-dimensional surface regions of rectangular and circular shape. In the following, these group of sensors are referred to 2D-arrays; this naming is used to emphasize their relation to two-dimensional (2D) surface shapes.

Through the characteristics of cylindrical spreading and the assumption of relatively constant material and plate thickness within a limited surface region, data from 2D-arrays (group of sensors) can be studied with almost the same technique as arrays defined by sensors along a line. Practically, this is carried out by analysing the data in the radial offset domain. In the radial offset domain, the $x - y$ coordinate of each sensor is converted to a spatial radial coordinate r that measures the distance from the sensor to the source location (acquired from reciprocity) in the centre of the measurement domain (red cross in Figure 6.9). That is, the radial offset domain represents a polar domain defined by a radial axis directed outwards from the location of the source (red cross in Figure 6.9).

An example of a 2D-array defined by a rectangular shape is shown with blue diamond markers in Figure 6.10(a). This rectangular 2D-array is defined by the slope of 25° and the width of 0.3 m. In total, this 2D-array contains 85 sensor. The data collected by these 85 sensors are further studied in the radial offset domain. The surface-in plane acceleration response (parallel to the radial axis) for the 85 sensors within the rectangular 2D-array are shown in Figure 6.10(b). This seismic plot shows the time history of each recorded signal. The displayed signals are sorted according to their location along the radial axis r. With aim of suppressing high frequency noise, a low-pass filter is applied in time domain to reduce the frequency content above 30 kHz. In similarity to the data presented in Figure 6.2(a), it is possible to observe the first arrival longitudinal wave, surface waves as well as the stationary S1-ZGV Lamb mode. That is, data from this 2D-array displayed in radial offset domain exhibit the same general full wave field characteristic as data obtained from arrays in the form of lines.

The use of a seismic plot is an efficient tool that provides an overview of measurement data in both time and space. Thus, both velocity (slope in Figure 6.10(b)) and frequency (periodicity in Figure 6.10(b)) may be estimated. However, since the recorded wave field consists of multi-modal and dispersive Lamb waves present simultaneously over a wide frequency range, reliable estimations of velocity and frequency may be challenging to acquire from the data in this representation. For this reason, it is useful to study the data in frequency domain. For an estimation of the spectral content

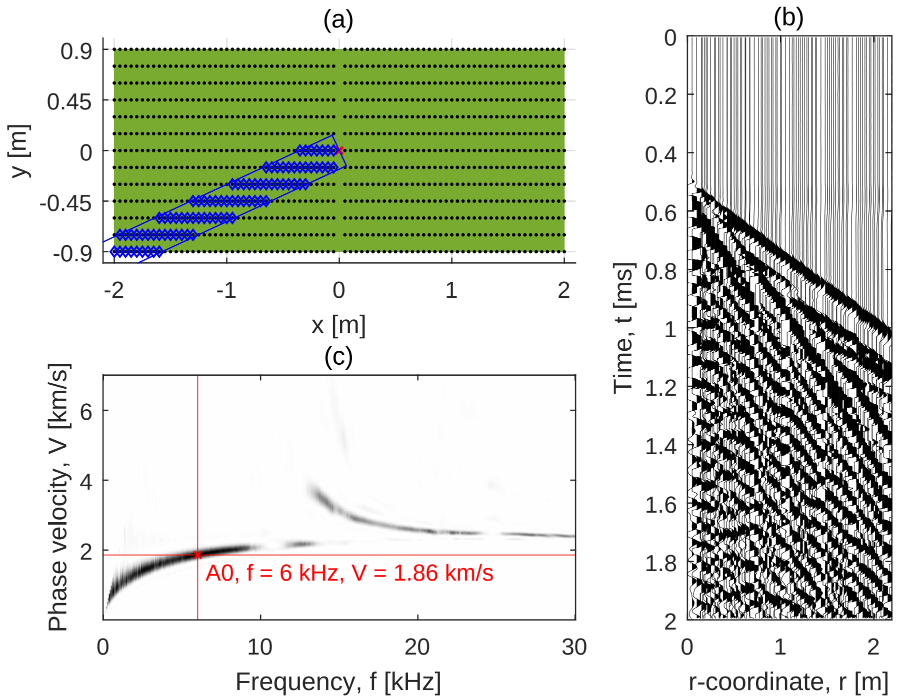

Figure 6.10: (a) Green rectangle: measurement domain. Black dots: sensors. Red cross: Source location. Rectangular 2D-array shown with blue diamond markers. (b) Low-pass filtered time domain data of surface in-plane (parallel to radial axis) acceleration response. (c) Frequency-phase velocity correlation image. Red cross shows the estimated phase velocity for A0 Lamb mode at 6 kHz.

of the recorded data from the 2D-array displayed in Figure 6.10(a), a two-dimensional Fourier transform is used to create an image that shows the spectral correlation for a range of frequency-phase velocity combinations. Such correlation image is shown in Figure 6.10(c). In Figure 6.10(c) the well-known pattern of the fundamental Lamb modes A0 and S0 is observed clearly (for instance, compare with Figure 3.6). This result ensures validity and strengthens the usefulness of 2D-arrays for Lamb wave evaluations performed in radial offset domain. Here, note that the processing that results in Figure 6.10(c) is essentially the same as that used in Paper I and Paper II; the difference is that a transformation of data into the radial offset domain must be performed at first.

Spectral estimations such as the one shown in Figure 6.10(c) can be used for analysis of the dispersive properties of the plate; this provides an indirect estimation of the material properties and thickness of the plate. For the 2D-array displayed with blue diamond markers in Figure 6.10(a), the estimated spectral content shown in the correlation image (Figure 6.10(c)) is representative for the surface region covered by the 2D-array. More specifically, the estimation represent a type of spatial average since the 2D-array can be interpreted as a spatial averaging operator dependent on the 2D-array surface size and shape. Nevertheless, since estimates as function of the region covered by the 2D-array are obtained, this can be utilized for monitoring of potential variation of material properties and thickness in the lateral plane of the plate. Accordingly, by estimating the dispersive properties at different locations of a plate, the homogeneity of a plate can be assessed.

Since the recorded data contains a full wave field response with a wide frequency bandwidth, an assessment of homogeneity may be focused on the full frequency range of the dispersive wave field. However, such analysis usually requires extensive work and may for this reason not be sensible for an initial assessment concerning homogeneity of a measurement object. Owing to this, it is reasonable to select one or a few modes at a narrow band of frequencies for the initial analysis of homogeneity. As example here, the A0 Lamb mode at the frequency 6 kHz is selected for further investigations. This mode is selected since its mode shape is present through the entire thickness of the plate. For this mode, the phase velocity is dependent on the material properties through the complete cross-sectional thickness. Moreover, the phase velocity is also dependent on the plate thickness. For the 2D-array shown in Figure 6.10(a), the estimated phase velocity for the A0 Lamb mode at 6 kHz is 1.86 km/s; this estimate is highlighted with a marking by the red cross in Figure 6.10(c). The wavelength of the A0 Lamb mode at 6 kHz is approximately $\lambda = V/f \approx 0.3$ m; by considering the wavelength λ in comparison with the nominal thickness (0.12 m) for the plate, it can be noticed that the mode is not expected to be sensitive for local material inhomogeneities such as reinforcement bars.

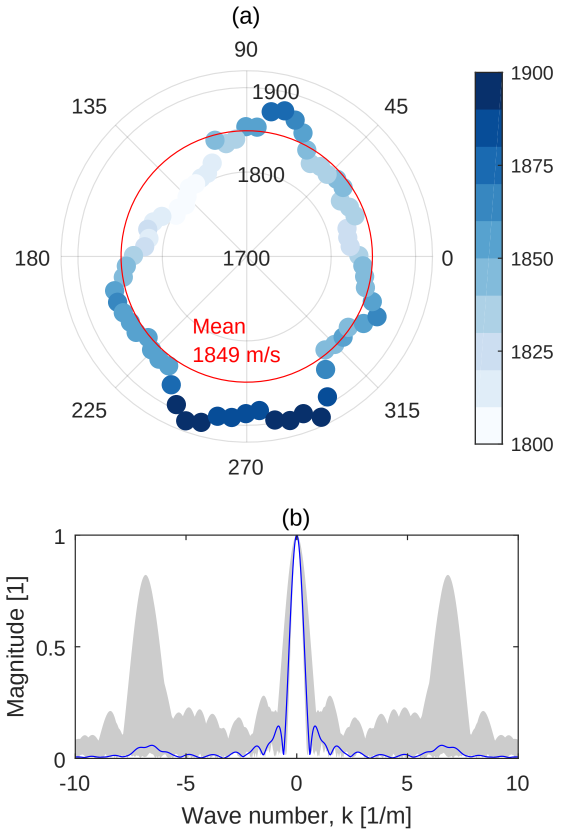

Figure 6.11: (a) Estimated phase velocity for the A0 Lamb mode at 6 kHz as function of polar angle for rectangular array shown in Figure 6.10(a). (b) Grey shading: envelope of normalized absolute value of the Fourier transform of the array window functions in frequency (wave number). Blue line represents the rectangular 2D-array in Figure 6.10(a).

Through a stepwise rotation of the 2D-array in Figure 6.10(a) around the measurement domain and at each step performing an estimation of the phase velocity as in Figure 6.10(c), the variation of phase velocity as function of polar angle can be mapped. For the A0 Lamb mode at 6 kHz, the result from such evaluation is shown in Figure 6.11(a). Results in Figure 6.11(a) show that an almost consistent phase velocity with little relative variation for the A0 Lamb mode at 6 kHz is observed. This verifies a homogeneous plate with essentially constant material and thickness within the studied measurement domain; this is expected since a newly cast plate is investigated. A slight difference in processing between line arrays and 2D-arrays exists. Usually, a uniform sampling in space domain is used for line arrays. However, for 2D-arrays this is usually not the case; typically a non-uniform sampling (sensor spacing) is used. This aspect slightly changes the numerical implementation of the discrete Fourier transform that creates the frequency-phase velocity correlation image (e.g. Figure 6.10(c)). Furthermore, to ensure reliability of the obtained results, the influence from sampling should also be considered. This can be realized by studying the Fourier transform of the spatial window corresponding to the array. Figure 6.11(b) shows the Fourier transforms of the spatial array windows. The study of these curves is of value since sampling in space domain (here, by means of the spatial 2D-array) corresponds to a convolution in frequency domain between the array, represented by a boxcar window function, and the true spectrum.

A rectangular 2D-array is not the only alternative for mapping of variation in dispersive properties. Another possibility is to use circular 2D-arrays. Such example is shown in Figure 6.12(a) by means of a circular 2D array with the radius of 0.45 m. Instead of a rotation, the 2D-array is swept within a rectangular grid space given by 40 points along the x axis and 20 points along the y axis. At each grid point, an estimation of the phase velocity for the A0 Lamb mode at 6 kHz is performed following the same technique as previously. The result from this mapping of phase velocity is shown in Figure 6.12(c) as a two-dimensional image plot. In Figure 6.12(c), each pixel corresponds to the location of a grid point in which an estimation of phase velocity is performed. Although the colour is assigned individually for each pixel, note that this colour (estimation) should not be interpreted as a pointwise estimate of the phase velocity; the estimated phase velocity is representative for the complete surface covered by the 2D-array, i.e. the estimate may be interpreted as a spatial average within the 2D-array surface.

In similarity with Figure 6.11(a), Figure 6.12(c) shows an almost consistent phase velocity for the A0 Lamb mode at 6 kHz. This result further verifies that a condition of homogeneous material and plate thickness is present within the measurement domain. Moreover, Figure 6.12(c) also demonstrates that mapped variation of phase velocity can be illustrated in a two-dimensional image plot and thereby serve as one example of a tool for assessment of homogeneity. From a general perspective, results also demonstrates the possibility of performing a new (for plate-like concrete structures) type of imaging analysis based on propagating Lamb waves from a full wave field dataset with wide frequency bandwidth. Since only a light and portable equipment is required and that the measurement can be performed in fairly short amount of time, it is expected that this technique is an interesting and valuable complement to existing imaging techniques based on e.g. ultrasonic pulse echo and synthetic apertures.

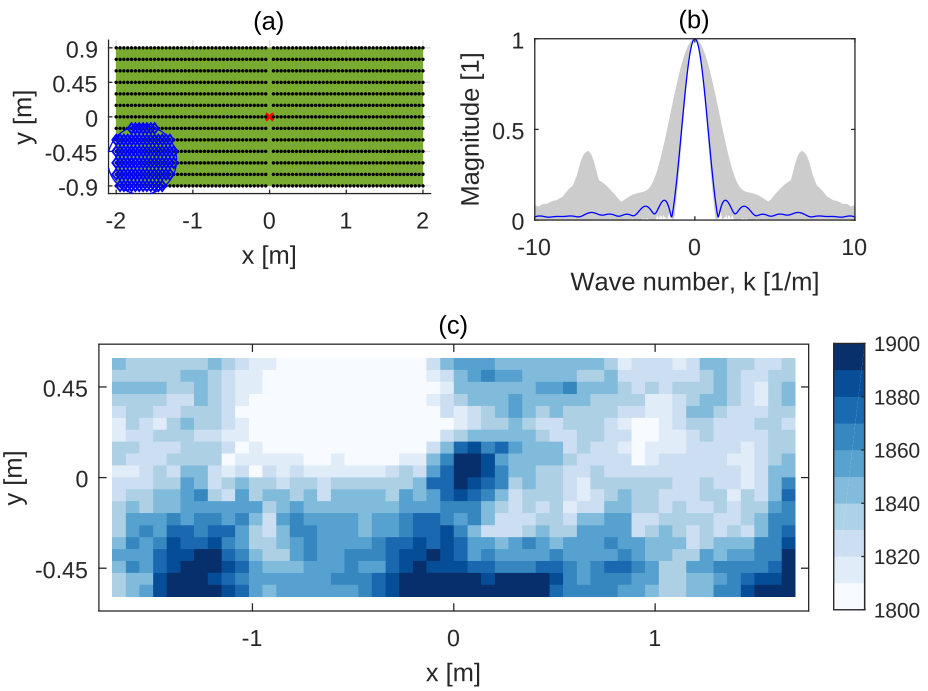

Figure 6.12: (a) Green rectangle: measurement domain. Black dots: sensors. Red cross: source location. Circular 2D-array shown with blue diamond markers. (b) Grey shading: envelope of normalized absolute value of the Fourier transform of the array window functions in frequency (wave number) domain. Blue line represents the circular 2D-array in top left sub-figure. (c) Estimated phase velocity for the A0 Lamb mode at 6 kHz as function of centre coordinate of circular 2D-array. Note that the pixels should not be interpreted as pointwise estimations due to the averaging effect from the 2D-array; the estimate is approximately representative to the region covered by the array.

6.3 Theoretical study inhomogeneous plates

In Paper I and Paper II, the presented work is based on the assumption of a homogeneous material in all directions for the complete domain of investigation; this assumption is implied from to the use of Lamb wave theory. The assumed condition of homogeneity is somewhat loosened in Paper III since a constant material and plate thickness is assumed only within a limited domain (the 2D-array); that is, homogeneity in the lateral plane of the plate is not assumed. However, as mentioned in Chapter 2, variations of the material properties *through* the thickness are observed for some concrete structures. Typically, such variations may manifest itself as a continuous variation of the acoustic bulk wave velocities. Such variations are in general not considered in testing of plate-like concrete structures with ZGV Lamb modes. This serves as the motivation for the work presented in Paper IV, in which the behaviour of the lowest (first) ZGV modes in two synthetic cases are investigated. In particular, important aspects of the investigation are whether a ZGV mode will appear, and if so, can it be detected with same robustness as for a homogeneous case, and also, how can the frequency of the ZGV mode be interpreted in relation to the material properties of the plate? To answer these questions, a semi-analytical finite element (SAFE) simulation as well as a conventional finite element simulation are performed.

The two cases, referred to as case 1 and case 2, are defined by two plates with inhomogeneous and non-symmetric continuous variation of the acoustic bulk wave velocities. Both cases are modifications of an isotropic reference case, which is represented by a linear elastic isotropic plate. Then, by the usage of two scaling functions, one for each case, the cases 1 and 2 are created by adjusting the acoustic bulk wave velocities (longitudinal wave velocity V_L and transversal wave velocity V_T) according to a scaling function with spatially varying amplitude along the plate thickness coordinate z. The scaling functions for cases 1 and 2 are shown in Figure 6.13(a) and Figure 6.13(b), respectively. The corresponding variations in the longitudinal and transversal wave velocities as function of the thickness coordinate for cases 1 and 2 are shown in Figure 6.13(c) and Figure 6.13(d), respectively.

It should be noted that cases 1 and 2 represent one selection among many potential candidate material variation cases; in fact, an infinite number of material variation cases exist, and naturally it is necessary to limit these cases. Cases 1 and 2 are selected to enable a study of ZGV modes in plates with a continuous inclusion of material with either high or low acoustic bulk wave velocities. It is anticipated that many concrete structures with one simple anomaly fall within the boundary limits formed by the definitions of cases 1 and 2 since these represent a fairly strong change in the acoustic velocities. Thus, it is expected that observed qualitative and quantitative re-

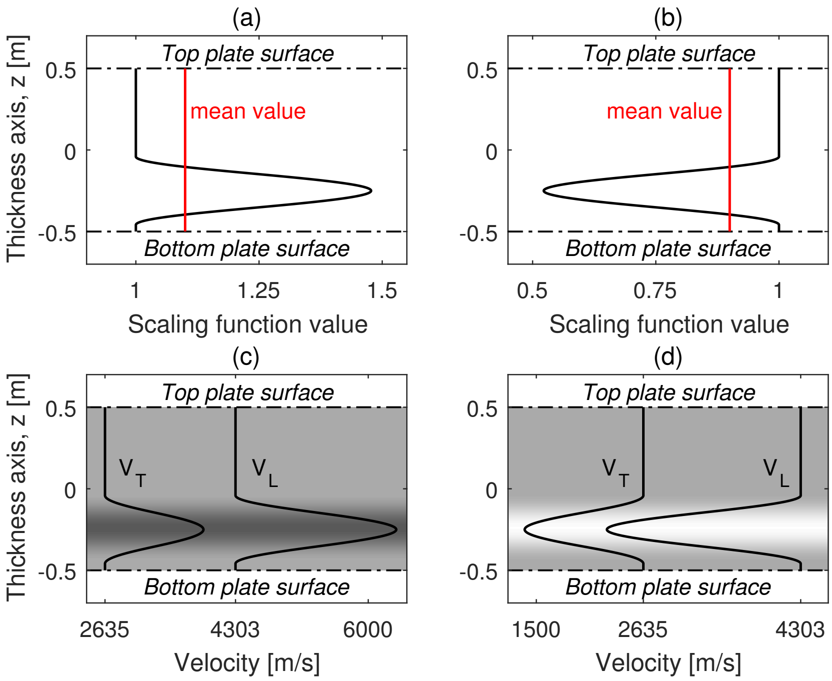

Figure 6.13: Scaling function for (a) case 1 and (b) case 2. The cases are characterised by a continuous variation of acoustic bulk wave velocities for. Cases 1 and 2 are show in (c) and (d), respectively. Cases 1 (c) and 2 (d) are created from a homogeneous isotropic reference case defined by a longitudinal wave velocity $V_L = 4303\,\mathrm{m/s}$, a transversal wave velocity $V_T = 2635\,\mathrm{m/s}$ (Poisson's ratio $\nu = 0.2$), and density $\rho = 2400\,\mathrm{kg/m^3}$ and the scaling functions in (a) and (b); by adjusting the acoustic bulk wave velocities (V_L and V_T) according to the scaling functions, cases 1 (c) and 2 (d) are created.

sults can be considered as valuable and relevant for other plate-like concrete structures as well.

The dispersion relations (curves) for cases 1 and 2 are calculated using a semi-analytical finite element (SAFE) model. Figure 6.14(a) and Figure 6.14(b) show the dispersion curves for the four lowest modes, denoted M1-M4, for the cases 1 and 2, respectively. For both cases, Figure 6.14 shows that the overall pattern exhibited by the M1-M4 modes is similar to the pattern exhibited by the A0, S0, A1, and S1 Lamb modes for the isotropic reference plate (dotted black lines). In similarity with the S1 dispersion curve for the isotropic reference case, Figure 6.14 shows that the M4 mode exhibit minimum points at a nonzero wave number. These minimum points represent modes at which the group velocity vanishes according to $V_g = df/dk = 0$; i.e., ZGV modes are observed also for cases 1 and 2. In the following, these modes (points) are referred to as M4-ZGV. However, although similarities exist between the M4-ZGV mode and the S1-ZGV, the cases 1 and 2 represent a condition with a complex relation between mode frequency and acoustic material velocity. In contrast to the isotropic case (Lamb waves), no simple relation between mode frequency and acoustic velocity exists. This condition of additional complexity compared to the isotropic case may lead to uncertainties in practical applications. For example, if an isotropic Lamb wave model is assumed under the actual condition of case 1 or 2, then the estimated acoustic material velocity or plate thickness from the M4-ZGV mode will be difficult to interpret since it is not representative to a mean value or other similar established quantitative measure.

To further study the M4-ZGV mode, the excitability is calculated. Figure 6.15(a) and Figure 6.15(b) show the excitability for the M1-M4 mode for cases 1 and 2, respectively. Figure 6.15(a) and (b) show that the M4 curve for both cases 1 and 2 exhibit high values of excitability around the M4-ZGV mode frequency. This is similar with the behaviour observed for S1 Lamb mode of the isotropic reference case. This means that high displacement amplitudes, in the form of a local resonance of the plate, are to be expected at the top plate surface even in for cases 1 and 2 by means of the M4-ZGV modes. The robustness and detectability of the M4-ZGV mode frequency is further studied in a simulation of a combined impact-echo and surface wave measurement; that is, this simulation corresponds to the applications in for example Paper I and Paper II. Results from this simulated application are shown in Figure 6.16(a) and (c), which shows the acceleration response as function of time at different radial offset distances to the hammer impact for cases 1 and 2, respectively. The time domain datasets are transformed to wave number frequency domain using a two-dimensional discrete Fourier transform. Figure 6.16(b) and (d) show the simulated response in presented in wave number frequency domain for the cases 1 and

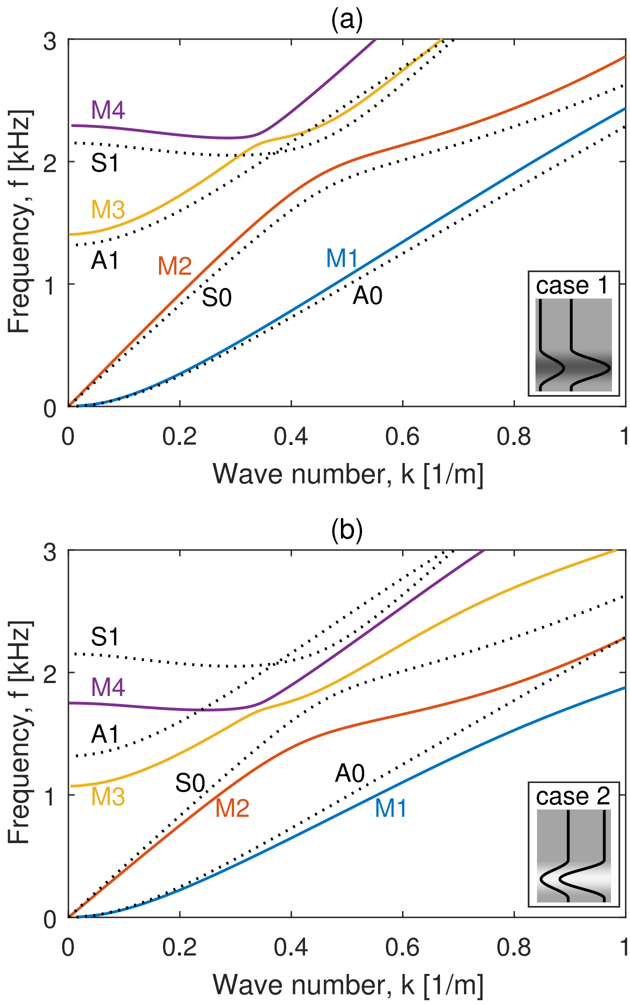

Figure 6.14: Dispersion curves for the four lowest modes M1-M4 for (a) case 1 and (b) case 2. The four lowest modes (A0, S0, A1, S1) for the isotropic reference case is shown with black dotted lines.

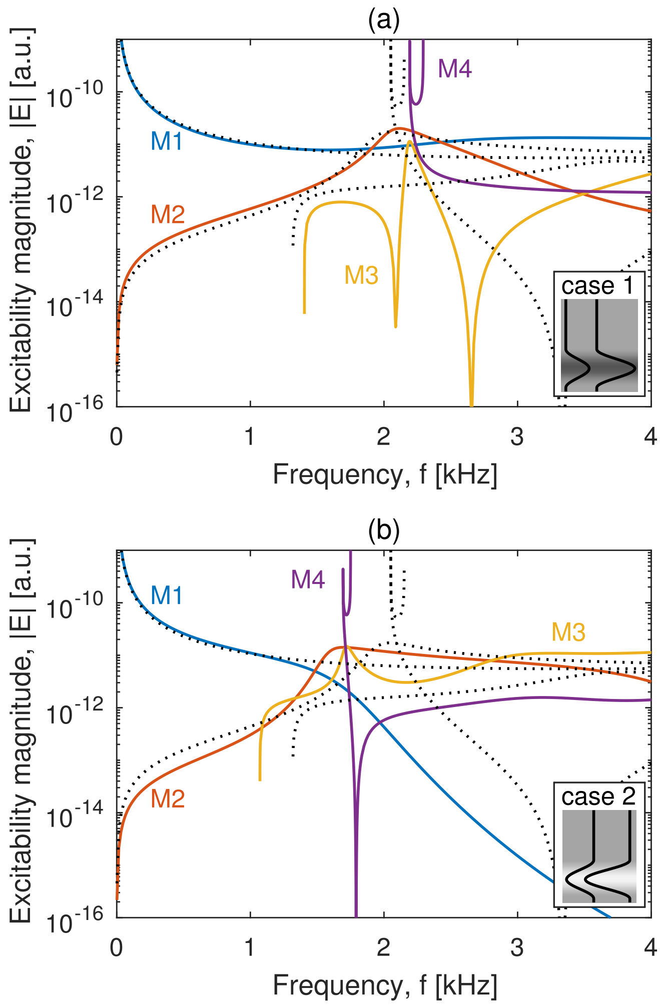

Figure 6.15: Excitability for (a) case 1 and (b) case 2. Solid lines in colour (M1-M4) represent the four lowest modes for cases 1 and 2. Dotted black lines show isotropic reference case. Here, excitability is interpreted as the displacement magnitude at the top surface of the plate in the surface normal direction, caused by a unit point load applied at the same point and direction. The excitability is calculated according to $E = i\omega|U|^2/(4P)$, where ω is the angular frequency, U is the surface normal displacement at the top surface of the plate, and P is the one-period time and cross-section-averaged Poynting vector component in the propagation direction of the mode.

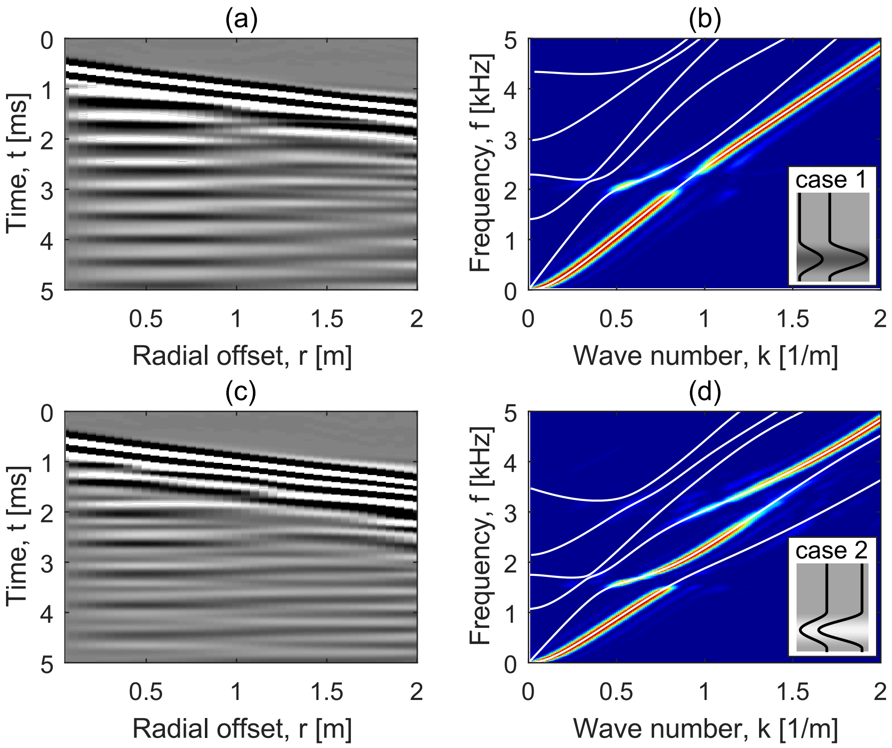

Figure 6.16: Simulated datasets for (a) case 1 and (c) case 2. Estimation of wave number-frequency content for (b) case 1 and (d) case 2 calculated using a 2D discrete Fourier transform. Superimposed dispersion curves from the SAFE analysis are shown as solid white lines.

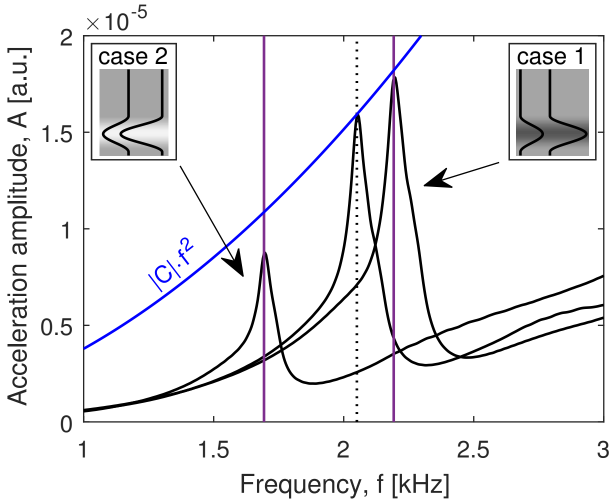

Figure 6.17: Discrete Fourier transform of summed acceleration response signals within 1 m distance from the impact source for case 1, case 2, and the isotropic reference case. Observed left and right peaks correspond to the M4-ZGV mode for cases 2 and 1, respectively. Middle peak corresponds to the S1-ZGV Lamb mode. The vertical lines indicate the predicted ZGV frequencies from the SAFE analysis; a good agreement is observed.

2, respectively. Figure 6.16(b) and (d) also show superimposed dispersion curves from the SAFE analysis as solid white lines. A good agreement between the dispersion curves and the dataset is observed for both cases; this serves as a verification of the correctness of the dispersion curves from the SAFE analysis. For cases 1 and 2, a differentiation of surface wave mode at high frequency is observed: the surface wave at high frequency is related to the M1 mode for case 1 and to the M3 mode for case 2, see Figure 6.16(b) and (d). This behaviour appears since the regions near the top and bottom surfaces are exposed to different mechanical properties (acoustic bulk wave velocities). If this behaviour is unknown or not considered, uncertainty and error in data evaluation may arise.

To study the detectability of the M4-ZGV mode for cases 1 and 2 in this simulated application, a discrete Fourier transform is calculated for the signals in vicinity of the impact source. Here, to facilitate identification of the M4-ZGV mode frequency by reducing the influence from propagating modes, the DFT is calculated on a summation of the signals within a radial distance of 1 m from the source. The absolute value of the spectrum from this calculation is shown in Figure 6.17. For reference, the frequencies corresponding to the M4-ZGV mode and the S1-ZGV Lamb mode from the SAFE analysis are marked with vertical lines: a good agreement can be observed for all cases. Figure 6.17 shows that the M4-ZGV mode materializes as a resonance with high amplitude at a distinct frequency, similar to the S1-ZGV Lamb mode. This is in line with the expected behaviour from the high modal excitability displayed in Figure 6.15. A slight variation in amplitude of the M4-ZGV mode between the cases is observed, which is expected to be dependent on at least two reasons. First, for a constant absolute displacement amplitude $|C|$ in frequency domain, the corresponding absolute acceleration amplitude is given by a quadratic parabola $|C|f^2$, see parabola in Figure 6.17. This makes the acceleration magnitude to increase with frequency for a constant displacement amplitude in frequency domain. Second, the top surfaces of the M4-ZGV mode for cases 1 and 2 are exposed to different material properties; this creates a slightly distorted modal shape compared to the S1-ZGV Lamb mode, and for this reason a variation in acceleration magnitude is generated between the cases. Still, the frequency of the peaks corresponding to the M4-ZGV mode is detected with the same robustness and accuracy as for the S1-ZGV Lamb mode. Nevertheless, results show that in this practical nondestructive application, ZGV modes can be used even for cases 1 and 2. It is expected that this result can be extended and generalized to other inhomogeneous plates that are within the boundary limits or similar to cases 1 and 2. Yet, since material variation typically leads to increased complexity in the relation between mode frequency and material properties, uncertainties in estimations may, depending on the magnitude of the inhomogeneity, occur.

Chapter 7

Conclusions

Near field effects lead to a systematically underestimated plate thickness in both conventional impact-echo testing and combined impact-echo and surface wave analysis of plate-like concrete structures. A main source of uncertainty is the interpretation of the first arrival wave velocity as the true longitudinal wave velocity. Alternative approaches for estimation of Poisson's ratio that are independent on the evaluation of first arrivals are therefore important. The proposed technique for estimation of Poisson's ratio based on the amplitude polarization of the S1-ZGV Lamb mode is one example of such approach. Unlike the cases when modes with different volume sensitivity are used, an estimate of Poisson's ratio representative for the complete plate cross-sectional thickness is obtained since the S1-ZGV Lamb mode is present through the entire plate thickness. For this approach applied in a practical measurement, an improved estimate of the nominal thickness is obtained compared to the case when Poisson's ratio is estimated from first arrivals.

A Lamb wave phase velocity imaging technique based on 2D arrays created from limited subdomains within the global measurement domain is presented with a measurement on a newly cast concrete plate as illustrating example. The novel aspect of this technique is the study of *propagating* waves in limited sub domains defined by the 2D arrays. Compared to conventional ultrasonic reflection imaging techniques, the 2D array technique is not limited to specific operating frequencies (transducers) since it is based on a full wave field dataset with wide-band frequency content. The technique operates at a lower frequency compared to ultrasonic approaches and is therefore expected to give a larger possible investigated volume and depth of penetration; this can be beneficial in evaluations of thick plate-like concrete structures. The 2D arrays are in this case used to map the variation of the phase velocity for the A0 Lamb mode. Results show a low variation of the estimated phase velocity; this verifies the condition of a relatively homogeneous material and plate thickness in the measurement domain. Whereas the proposed 2D array technique is applicable for monitoring of variations in the lateral plane of a plate, results in the literature report that material variation may also exist transversally through the thickness of concrete structures. For this reason, a theoretical study is conducted to improve the understanding of non-destructive evaluation techniques based on zero-group velocity (ZGV) modes. Limited to a study of the lowest zero-group velocity mode, two cases with material variation through the plate thickness are investigated using a semi-analytical finite element (SAFE) model and a simulated non-destructive application. It is found that for both material variation cases a ZGV mode similar to the S1-ZGV for homogeneous plates exists. The detectability and robustness of this ZGV mode is found to be comparable and similar to the S1-ZGV for homogeneous plates. That it is, evaluation techniques utilizing the lowest ZGV mode are applicable also for these two material variation cases.

Chapter 8

Suggestions for further work

The measurements in this thesis (Paper I, Paper II and Paper III) are performed on a limited number of test sites and with the maximum plate thickness of 0.5 m. Given the aim and objective of this thesis, see Section 1.3, it is of importance to investigate the applicability at more test sites which preferably should be thick (>1 m) plate-like concrete structures. Such studies may also, for instance, include investigations of sensitivity for boundary effects for the amplitude polarization technique (Paper II) and exploration of mode sensitivity for defects or anomalies for the 2D array technique (Paper III).

Results in Paper I show that near-field effects and the estimation of longitudinal wave velocity from first arrivals may influence evaluations based on point-source excitation from e.g. hammer impacts. Although these results provide a step towards increased understanding of the wave-field behaviour, a full interpretation and explanation of these effects still remains an unsolved matter (according to the author). For further investigations of near-field effects it is anticipated that simulations using semi-analytical finite element models (see Paper IV) may be useful in this process. However, to the author's experience an implementation outside the FE-code of COMSOL (COMSOL Inc., 2016) would in such cases be useful for improved flexibility and control. This is related to that the implementation of a SAFE simulation in COMSOL implies a translation/transformation of the SAFE matrix expressions to a general eigenvalue equation form (Predoi et al., 2007).

The new approach for estimation of Poisson's ratio based on the amplitude polarization of the S1-ZGV Lamb mode proposed in Paper II highlights the potential of multicomponent measurements. For future work it is suggested that focus may be directed on extracting more information from such multicomponent measurements; for instance, in a related publication (Baggens and Ryden, 2015c), results show that the A2-ZGV Lamb mode can be identified by analysing the surface-in plane response. Here, it is anticipated that an investigation (e.g. using semi-analytical finite element simulations) of the A2-ZGV Lamb mode in more detail could be useful for improved understanding. Another prospective alternative for further studies could be to investigate the phase aspect between the surface in-plane and surface normal component.

The 2D array technique presented in Paper III is demonstrated on a newly cast and ideally homogeneous plate. For further investigations it is important to study the applicability of the technique in cases with potential anomalies and defects. Moreover, the 2D arrays are based on data recorded in a rectangular grid. It is emphasized that this rectangular grid is not a condition required to enable 2D arrays. Sparse impact locations at arbitrary positions works equally well in this technique; the important matter is that the location of an impact (signal) must be known, but the exact location of the impact itself is not the critical aspect. Consequently, the 2D array technique would benefit greatly by developing a system that can locate the position of the hammer impact when the impact is performed; i.e. the opposite from the case in Paper III where the impact is performed at the pre-defined location by a marking. Another idea for further developments of 2D arrays concerns imaging in the transversal plane of the plate, e.g. see the SAFT images from synthetic impact-echo data in (Schubert and Köhler, 2008; Ganguli et al., 2012).

It is expected that developments concerning the measurement equipment used in this thesis may be possible. For instance, implementation of wireless devices is one such example. Moreover, the concept of air-coupled source generation and detection is also one alternative. Another interesting alternative is to study the possibility of using augmented reality devices. For instance, eye-glasses for augmented reality and digital image processing techniques could be one alternative approach for providing an operator with direct instructions and feedback in the practical execution of non-destructive measurements.

Chapter 9

Bibliography

O. Abraham, C. Leonard, P. Cote, and B. Piwakowski. Time frequency analysis of impact-echo signals: numerical modeling and experimental validation. *ACI Materials journal*, (97):645–657, 2000. DOI: 10.14359/9978.

O. Abraham, J. S. Popovics, and L.-M. Cottineau. Modification of the zero group velocity (impact echo) resonance frequency in the presence of voids for the inspection of tendon ducts. In *AIP Conference Proceedings*, volume 1365, pages 1365–1370, 2011. DOI: 10.1063/1.3592091.

O. Abraham, B. Piwakowski, G. Villain, and O. Durand. Non-contact, automated surface wave measurements for the mechanical characterisation of concrete. *Construction and Building Materials*, 37:904–915, 2012. ISSN 09500618. DOI: 10.1016/j.conbuildmat.2012.03.015.

J. D. Achenbach. *Wave Propagation in Elastic Solids*. North-Holland Publishing Company, 1973.

D. Algernon and H. Wiggenhauser. Impact Echo Data Analysis Based on Hilbert-Huang Transform. *Transportation Research Record*, 2028(-1):146–153, dec 2007. ISSN 0361-1981. DOI: 10.3141/2028-16.

D. Alleyne and P. Cawley. A two-dimensional Fourier transform method for the measurement of propagating multimode signals. *The Journal of the Acoustical Society of America*, 89(3):1159–1168, mar 1991. ISSN 0001-4966. DOI: 10.1121/1.400530.

H. Almansouri, C. Johnson, D. Clayton, Y. Polsky, C. Bouman, and H. Santos-Villalobos. Progress implementing a model-based iterative reconstruction algorithm for ultrasound imaging of thick concrete. *AIP Conference Proceedings*, 1806, 2017. ISSN 15517616. DOI: 10.1063/1.4974557.

ASTM C 1383. Standard Test Method for Measuring the P-Wave Speed and the Thickness of Concrete Plates Using the Impact-Echo Method, Annual Book of American Society for Testing and Materials (ASTM) Standards.

B. Auld. *Acoustic Fields and Waves in Solids, Vol. II.* Robert E. Krieger Publishing Company, Malabar, Florida, 2nd edition, 1990.

O. Baggens and N. Ryden. Systematic errors in Impact-Echo thickness estimation due to near field effects. *NDT & E International*, 69:16–27, jan 2015a. ISSN 09638695. DOI: 10.1016/j.ndteint.2014.09.003.

O. Baggens and N. Ryden. Near field effects and estimation of Poisson's ratio in impact-echo thickness testing. In *41st annual Review of Progress in Quantitative Non-Destructive Evaluation*, volume 34, pages 1415–1422, 2015b. ISBN 9780735412927. DOI: 10.1063/1.4914757.

O. Baggens and N. Ryden. Lamb Wave Plate Parameters from Combined Impact-Echo and Surface Wave Measurement. In *Non-Destructive Testing in Civil Engineering (NDT-CE 2015)*, pages 30–38, Berlin, Germany, 2015c. NDT.net. ISBN 4646222000.

O. Baggens and N. Ryden. Poisson's ratio from polarization of acoustic zero-group velocity Lamb mode. *The Journal of the Acoustical Society of America*, 138(1):EL88–EL92, jul 2015d. ISSN 0001-4966. DOI: 10.1121/1.4923015.

C. L. Barnes and J.-F. Trottier. Hybrid analysis of surface wavefield data from Portland cement and asphalt concrete plates. *NDT & E International*, 42(2):106–112, mar 2009. ISSN 09638695. DOI: 10.1016/j.ndteint.2008.10.003.

I. Bartoli, A. Marzani, F. Lanza di Scalea, and E. Viola. Modeling wave propagation in damped waveguides of arbitrary cross-section. *Journal of Sound and Vibration*, 295(3-5):685–707, 2006. ISSN 0022460X. DOI: 10.1016/j.jsv.2006.01.021.

A. Bayon, F. Gascon, and F. J. Nieves. Estimation of dynamic elastic constants from the amplitude and velocity of Rayleigh waves. *The Journal of the Acoustical Society of America*, 117(6):3469–3477, 2005. ISSN 00014966. DOI: 10.1121/1.1898663.

L. Bodet, O. Abraham, and D. Clorennec. Near-offset effects on Rayleigh-wave dispersion measurements: Physical modeling. *Journal of Applied Geophysics*, 68(1):95–103, may 2009. ISSN 09269851. DOI: 10.1016/j.jappgeo.2009.02.012.

D. Boiero, P. Bergamo, R. B. Rege, and L. V. Socco. Estimating surface-wave dispersion curves from 3D seismic acquisition schemes : Part 1 — 1D models. *Geophysics*, 76(6):G85–G93, 2012. ISSN 00168033. DOI: 10.1190/geo2011-0124.1.

A. Boyd and C. Ferraro. Effect of curing and deterioration on stress wave velocities in concrete. *Journal of materials in civil engineering*, (April): 153–158, 2005. DOI: 10.1061/(ASCE)0899-1561(2005)17:2(153).

J. Bungey, S. Millard, and M. Grantham. *Testing of Concrete in Structures*. Taylor & Francis, Abingdon, 4 edition, 2006. ISBN 978–0–415–26301–6.

M. Castaings, C. Bacon, B. Hosten, and M. V. Predoi. Finite element predictions for the dynamic response of thermo-viscoelastic material structures. *The Journal of the Acoustical Society of America*, 115(3):1125–1133, 2004. ISSN 00014966. DOI: 10.1121/1.1639332.

M. Cees, D. Clorennec, D. Royer, and C. Prada. Edge resonance and zero group velocity Lamb modes in a free elastic plate. *The Journal of the Acoustical Society of America*, 130(2):689–94, aug 2011. ISSN 1520-8524. DOI: 10.1121/1.3607417.

M. Cès, D. Clorennec, D. Royer, and C. Prada. Thin layer thickness measurements by zero group velocity Lamb mode resonances. *The Review of scientific instruments*, 82(11):114902, nov 2011. ISSN 1089-7623. DOI: 10.1063/1.3660182.

M. Cès, D. Royer, and C. Prada. Characterization of mechanical properties of a hollow cylinder with zero group velocity Lamb modes. *The Journal of the Acoustical Society of America*, 132(1):180–5, jul 2012. ISSN 1520-8524. DOI: 10.1121/1.4726033.

D. Clorennec, C. Prada, and D. Royer. Local and noncontact measurements of bulk acoustic wave velocities in thin isotropic plates and shells using zero group velocity Lamb modes. *Journal of Applied Physics*, 101(3): 034908, feb 2007. ISSN 0021-8979. DOI: 10.1063/1.2434824.

COMSOL Inc. COMSOL Multiphysics (r), 2016. URL `http://www.comsol.com`.

X. Dai, J. Zhu, and M. R. Haberman. A focused electric spark source for non-contact stress wave excitation in solids. *Journal of the Acoustical Society of America*, 134(6, 1):EL513–EL519, 2013. ISSN 0001-4966. DOI: 10.1121/1.4826913.

J. A. Deacon, C. L. Monismith, and J. T. Harvey. Pay Factors for Asphalt-Concrete Construction: Effect of Construction Quality on Agency Costs.

Technical report, Pavement Research Center, Institute of Transportation Studies, University of California, Berkeley, 1997.

J. Ditri, A. Pilarski, B. Pavlakovic, and J. Rose. Generation of guided waves in a plate by axisymmetric normal surface loading. *Review of Progress in Quantitative Nondestructive Evaluation*, 13A, 1994.

A. Ganguli, C. M. Rappaport, D. Abramo, and S. Wadia-Fascetti. Synthetic aperture imaging for flaw detection in a concrete medium. *NDT and E International*, 45(1):79–90, 2012. ISSN 09638695. DOI: 10.1016/j.ndteint.2011.09.004.

A. Garbacz, T. Piotrowski, L. Courard, and L. Kwaśniewski. On the evaluation of interface quality in concrete repair system by means of impact-echo signal analysis. *Construction and Building Materials*, 134:311–323, mar 2017. ISSN 09500618. DOI: 10.1016/j.conbuildmat.2016.12.064.

A. Gibson. *Advances in Nondestructive Testing of Concrete Pavements*. Ph.d. thesis, University of Illinois, 2004.

A. Gibson and J. S. Popovics. Lamb Wave Basis for Impact-Echo Method Analysis. *Journal of Engineering Mechanics*, 131(4):438–443, apr 2005. ISSN 0733-9399. DOI: 10.1061/(ASCE)0733-9399(2005)131:4(438).

K. F. Graff. *Wave Motion in Elastic Solids*. Dover Publications, New York, 1975. ISBN 0-486-66745-6.

M. Grohmann, E. Niederleithinger, and S. Buske. Geometry determination of a foundation slab using the ultrasonic echo technique and geophysical migration methods. *Journal of Nondestructive Evaluation*, 35(1):1–13, 2016. ISSN 15734862. DOI: 10.1007/s10921-016-0334-z.

M. Grohmann, S. Müller, E. Niederleithinger, and S. Sieber. Reverse time migration: introducing a new imaging technique for ultrasonic measurements in civil engineering. *Near Surface Geophysics*, 15(3):242–258, 2017. DOI: 10.3997/1873-0604.2017006.

J. B. Harley and J. M. F. Moura. Sparse recovery of the multimodal and dispersive characteristics of Lamb waves. *The Journal of the Acoustical Society of America*, 133(5):2732–2745, 2013. ISSN 0001-4966. DOI: 10.1121/1.4799805.

J. S. Heisey, K. H. Stokoe, and A. H. Meyer. Moduli of pavement systems from spectral analysis of surface waves. Technical report, Transportation Research Record 852, Transportation Research Board, Washington, D.C., 1982.

S. D. Holland and D. E. Chimenti. Air-coupled acoustic imaging with zero-group-velocity Lamb modes. *Applied Physics Letters*, 83(13):2704–2706, 2003. ISSN 00036951. DOI: 10.1063/1.1613046.

B. Hosten and M. Castaings. FE modeling of Lamb mode diffraction by defects in anisotropic viscoelastic plates. *NDT & E International*, 39(3): 195–204, apr 2006. ISSN 09638695. DOI: 10.1016/j.ndteint.2005.07.006.

M. Hu, Y. Lin, and C. Cheng. Method for Determining Internal P-Wave Speed and Thickness of Concrete Plates. *ACI Materials Journal*, 103(5): 327–335, 2006. ISSN 0889-325X. DOI: 10.14359/18154.

E. Kausel. Number and location of zero-group-velocity modes. *The Journal of the Acoustical Society of America*, 131(5):3601–10, may 2012. ISSN 1520-8524. DOI: 10.1121/1.3695398.

W. Ke, M. Castaings, and C. Bacon. 3D finite element simulations of an air-coupled ultrasonic NDT system. *NDT & E International*, 42(6):524–533, sep 2009. ISSN 09638695. DOI: 10.1016/j.ndteint.2009.03.002.

D. Kim, W. Seo, and K. Lee. IE-SASW method for nondestructive evaluation of concrete structure. *NDT & E International*, 39(2):143–154, mar 2006. ISSN 09638695. DOI: 10.1016/j.ndteint.2005.06.009.

P.-L. Liu, L.-C. Lin, Y.-Y. Hsu, C.-Y. Yeh, and P.-L. Yeh. Recognition of rebars and cracks based on impact-echo phase analysis. *Construction and Building Materials*, 142:1–6, jul 2017. ISSN 09500618. DOI: 10.1016/j.conbuildmat.2017.02.102.

V. Malhotra and N. Carino. *Handbook on Nondestructive Testing of Concrete*. CRC Press, Boca Raton, Florida, 2nd edition, 2004. ISBN 0-8493-1485-2.

K. R. Maser. Non-Destructive Measurement of Pavement Layer Thickness. *Final Report Caltrans No. 65A0074*, 2003.

R. Medina and A. Bayón. Elastic constants of a plate from impact-echo resonance and Rayleigh wave velocity. *Journal of Sound and Vibration*, 329(11):2114–2126, may 2010. ISSN 0022460X. DOI: 10.1016/j.jsv.2009.12.026.

R. Medina and M. Garrido. Improving impact-echo method by using cross-spectral density. *Journal of Sound and Vibration*, 304(3-5):769–778, jul 2007. ISSN 0022460X. DOI: 10.1016/j.jsv.2007.03.019.

S. Mezil, F. Bruno, S. Raetz, J. Laurent, D. Royer, and C. Prada. Investigation of interfacial stiffnesses of a tri-layer using Zero-Group Velocity Lamb modes. *The Journal of the Acoustical Society of America*, 138(5): 3202–3209, 2015. ISSN 0001-4966. DOI: 10.1121/1.4934958.

S. Müller, E. Niederleithinger, and T. Bohlen. Reverse Time Migration: A Seismic Imaging Technique Applied to Synthetic Ultrasonic Data. *International Journal of Geophysics*, 2012:1–7, 2012. ISSN 1687-885X. DOI: 10.1155/2012/128465.

A. Neville and J. Brooks. *Concrete Technology*. Prentice-Hall, Harlow, England, 2 edition, 2010. ISBN 978-0-273-73219-8.

M. Ohtsu and T. Watanabe. Stack imaging of spectral amplitudes based on impact-echo for flaw detection. *NDT and E International*, 35(3):189–196, 2002. ISSN 09638695. DOI: 10.1016/S0963-8695(01)00045-7.

C. B. Park, R. D. Miller, and J. Xia. Multichannel analysis of surface waves. *Geophysics*, 64(3):800–808, may 1999. ISSN 0016-8033. DOI: 10.1190/1.1444590.

G. F. Pla-Rucki and M. O. Eberhard. Imaging of Reinforced Concrete: State-of-the-Art Review. *Journal of Infrastructure Systems*, 1(2):134–141, 1995. ISSN 1076-0342. DOI: 10.1061/(ASCE)1076-0342(1995)1:2(134).

J. Popovics, W. Song, J. D. Achenbach, J. H. Lee, and R. F. Andre. One-sided stress wave velocity measurement in concrete. *Journal of Engineering Mechanics*, 124(12):1346–1353, dec 1998. ISSN 0733-9399. DOI: 10.1061/(ASCE)0733-9399(1998)124:12(1346).

J. Popovics, G. Cetrangolo, and N. Jackson. Experimental Investigation of Impact-Echo Method for Concrete Slab Thickness Measurement. *Journal of the Korean Society for Nondestructive Testing*, Vol 26(No 6):427–439, 2006.

J. Popovics, N. Ryden, and A. Gibson. New Developments in Nde Methods for Pavements. *Review of Quantitative Nondestructive Evaluation*, 27: 1320–1327, 2008. DOI: 10.1063/1.2902587.

S. Popovics. Effects of uneven moisture distribution on the strength of and wave velocity in concrete. *Ultrasonics*, 43(6):429–434, may 2005. ISSN 0041624X. DOI: 10.1016/j.ultras.2004.09.007.

C. Prada, D. Clorennec, and D. Royer. Local vibration of an elastic plate and zero-group velocity Lamb modes. *The Journal of the Acoustical Society of America*, 124(1):203–212, jul 2008. ISSN 1520-8524. DOI: 10.1121/1.2918543.

M. V. Predoi, M. Castaings, B. Hosten, and C. Bacon. Wave propagation along transversely periodic structures. *The Journal of the Acoustical Society of America*, 121(April):1935–1944, 2007. ISSN 00014966. DOI: 10.1121/1.2534256.

L. Qixian and J. Bungey. Using compression wave ultrasonic transducers to measure the velocity of surface waves and hence determine dynamic modulus of elasticity for concrete. *Construction and building materials*, 10(4):237–242, 1996. DOI: 10.1016/0950-0618(96)00003-7.

J. Roesset. Nondestructive dynamic testing of soils and pavements. *Tamkang Journal of Science and Engineering*, 1(2):61–80, 1998.

J. Roesset, D. Chang, K. Stokoe, and M. Aouad. Modulus and Thickness of the Pavement Surface Layer from SASW Tests. *Transportation Research Record*, (1260):53–63, 1990.

N. Ryden. Enhanced impact echo frequency peak by time domain summation of signals with different source receiver spacing. *Smart Structures and Systems*, 17(1):59–72, jan 2016. ISSN 1738-1584. DOI: 10.12989/sss.2016.17.1.059.

N. Ryden and M. Castaings. An Adaptive Frequency Domain Finite Element Model for Surface Wave Testing of Pavements. *AIP Conference Proceedings*, 1481(2009):1481–1488, 2009. DOI: 10.1063/1.3114132.

N. Ryden and C. B. Park. A combined multichannel impact echo and surface wave analysis scheme for non-destructive thickness and stiffness evaluation of concrete slabs. *AS NT, 2006 NDE Conference on Civil Engineering*, pages 247–253, 2006.

M. Sansalone. Impact-echo: the complete story. *ACI Structural Journal*, 94 (6):777–786, 1997. ISSN 08893241. DOI: 10.14359/9737.

M. Sansalone and W. Streett. *Impact-echo: Non-destructive Evaluation of Concrete and Masonry*. Bullbrier Press, 1997.

M. Schickert and M. Krause. Ultrasonic techniques for evaluation of reinforced concrete structures. In *Non-Destructive Evaluation of Reinforced Concrete Structures*, pages 490–530. Elsevier, 2010. DOI: 10.1533/9781845699604.2.490.

M. Schickert, M. Krause, and W. Müller. Ultrasonic Imaging of Concrete Elements Using Reconstruction by Synthetic Aperture Focusing Technique. *Journal of Materials in Civil Engineering*, 15(3):235–246, 2003. ISSN 0899-1561. DOI: 10.1061/(ASCE)0899-1561(2003)15:3(235).

F. Schubert and B. Köhler. Ten Lectures on Impact-Echo. *Journal of Nondestructive Evaluation*, 27(1-3):5–21, jul 2008. ISSN 0195-9298. DOI: 10.1007/s10921-008-0036-2.

F. Schubert, H. Wiggenhauser, and R. Lausch. On the accuracy of thickness measurements in impact-echo testing of finite concrete specimens–numerical and experimental results. *Ultrasonics*, 42(1-9):897–901, apr 2004. ISSN 0041-624X. DOI: 10.1016/j.ultras.2004.01.076.

V. Shevaldykin, A. Samokrutov, and V. Kozlov. Ultrasonic low-frequency transducers with dry dot contact and their applications for evaluation of concrete structures. In *2002 IEEE Ultrasonics Symposium, 2002. Proceedings.*, volume 00, pages 793–798. IEEE, 2002. ISBN 0-7803-7582-3. DOI: 10.1109/ULTSYM.2002.1193518.

S. W. Shin, C. B. Yun, J. S. Popovics, and J. H. Kim. Improved Rayleigh Wave Velocity Measurement for Nondestructive Early-Age Concrete Monitoring. *Research in Nondestructive Evaluation*, 18(1):45–68, jan 2007. ISSN 0934-9847. DOI: 10.1080/09349840601128762.

P. Shokouhi. Two-channel Impact-Echo. In *Non-Destructive Testing in Civil Engineering (NDT-CE 2009)*, Nantes, France, 2009. URL `http://ndt.net/article/ndtce2009/papers/102.pdf`.

P. J. Shull. *Nondestructive Evaluation - Theory, Techniques, and Applications*. M. Dekker, New York, 2002. ISBN 0-8247-8872-9.

O. Tofeldt and N. Ryden. Zero-group velocity modes in plates with continuous material variation through the thickness. *The Journal of the Acoustical Society of America*, 141(5):3302–3311, 2017. ISSN 0001-4966. DOI: 10.1121/1.4983296.

F. Treyssède and L. Laguerre. Numerical and analytical calculation of modal excitability for elastic wave generation in lossy waveguides. *The Journal of the Acoustical Society of America*, 133(June):3827–37, jun 2013. ISSN 1520-8524. DOI: 10.1121/1.4802651.

P. Turgut and O. F. Kucuk. Comparative relationships of direct, indirect, and semi-direct ultrasonic pulse velocity measurements in concrete. *Russian Journal of Nondestructive Testing*, 42(11):745–751, 2006. ISSN 1061-8309. DOI: 10.1134/S1061830906110064.

I. A. Viktorov. *Rayleigh and Lamb Waves Physical Theory and Applications*. Plenum Press, New York, 1967.

H. Wiggenhauser, A. Samokrutov, K. Mayer, M. Krause, S. Alekhin, and V. Elkin. Large Aperture Ultrasonic System for Testing Thick Concrete Structures. *Journal of Infrastructure Systems*, 23(1):B4016004, 2016. ISSN 1076-0342. DOI: 10.1061/(ASCE)IS.1943-555X.0000314.

T. Wu, J. Fang, G. Liu, and M. Kuo. Determination of elastic constants of a concrete specimen using transient elastic waves. *The Journal of the Acoustical Society of America*, 98(4):2142–2148, 1995.

J. Zhu and J. S. Popovics. Imaging Concrete Structures Using Air-Coupled Impact-Echo. *Journal of Engineering Mechanics*, 133(6):628–640, jun 2007. ISSN 0733-9399. DOI: 10.1061/(ASCE)0733-9399(2007)133:6(628).

D. Zywicki and G. Rix. Mitigation of near-field effects for seismic surface wave velocity estimation with cylindrical beamformers. *Journal of Geotechnical and Geoenvironmental ...*, (August):970–977, 2005. DOI: 10.1061/(ASCE)1090-0241(2005)131:8(970).

Appendices